Decision Making Advances

Journal homepage: www.dma-journal.org
ISSN: 2956-2384

Acceleration and Regenerative Braking Energy of Electric Trains: A Review for Energy-Management Decision Making

Szabolcs Fischer[1,*]

[1] Department of Transport Infrastructure and Water Resources Engineering, Széchenyi István University, Győr, Hungary

ARTICLE INFO

Article history:
Received 5 March 2026
Received in revised form 7 May 2026
Accepted 14 July 2026
Available online 18 July 2026

Keywords:
Railway; Electric locomotive; Electric engine; Electric multiple unit (EMU); Electric train; Acceleration energy; Regenerative braking energy; Recuperated energy; Energy measurement; Energy calculation; Network receptivity.

ABSTRACT

Optimizing traction energy is central to decarbonizing electrified railways, where two quantities dominate a train's electricity balance: energy consumed during acceleration and recovered during regenerative (recuperative) braking. Both are based on calculations or measurements, yet inconsistent definitions, metering boundaries, and reporting conventions make published values difficult to compare for energy-management decision-making. This paper reviews the possibilities for calculating and measuring electric locomotives and multiple units across 100 publications. A two-axis framework crosses energy type with analytical task, cross-cut by alternating versus direct-current supply and locomotive-hauled versus distributed-traction trains. For acceleration, it covers the multiplicative correction-factor method, effective mass and running resistance formulations, traction-measuring cars, onboard logging, optical character recognition, inertial sensors, and machine learning. For regeneration, it contrasts analytical, simulation-based, and data-driven calculations with onboard, wayside, and hybrid measurements, network receptivity, and usable energy. Measured energy depends strongly on sampling rate and metering boundary; wayside measurements underestimate recovery on direct-current systems; multiple units recover more efficiently than locomotive-hauled trains; and driving style and timetable structure dominate. Representative magnitudes recur: acceleration-energy correction factors of about 1.3 (range ≈1.25–1.5), regenerative-chain efficiencies of roughly 0.70–0.85, and recoverable braking energy of 10–30% of traction energy. The chief obstacle to comparability and reliable decision-making is methodological rather than technological; high-frequency, position-synchronized measurement, multi-train simulation, train-specific efficiency data, and harmonized metrics define best practice.

1. Introduction

Decarbonization of the transport sector is a central objective of contemporary energy and climate policy, and railway transport occupies a privileged position within it because of its comparatively low energy intensity and emissions per passenger- or tonne-kilometer [1–3]. Comparative life-cycle and operational analyses consistently place electrified railway ahead of road and air modes on these

* *Corresponding author.*
E-mail address: fischersz@sze.hu

https://doi.org/10.31181/dma412026186

metrics [4, 5], and the electrification of new and existing lines is widely pursued as part of long-term sustainability strategies [6]. Nevertheless, electric railways remain large consumers of electrical energy, particularly in high-frequency urban networks and in intercity and heavy-haul operation, so the efficient use of traction energy is a key operational and economic goal for infrastructure managers and operators [7–9].

The operational electricity balance of an electric train is conventionally decomposed into traction energy (positive), regenerative – equivalently, recuperated – braking energy (negative) and auxiliary energy for onboard services such as heating, ventilation, air conditioning, lighting, and so on. Two quantities govern the dynamic part of this balance and are the focus of the present review. The first is the energy consumed during acceleration. Because the traction system must rapidly build up kinetic energy, the acceleration phase is the most energy-intensive and thermodynamically demanding mode of operation, drawing high currents under transient electrical conditions that differ fundamentally from those of steady-state cruising (i.e., hauling at constant speed, without accelerating) [10]. The second is the energy recovered during braking through regeneration, in which the traction motors operate as generators, converting part of the train's kinetic energy back into electrical energy. Depending on operating conditions and network configuration, regenerative braking energy can account for roughly 10–30% of traction energy consumption [11, 12], so its efficient utilization is a substantial opportunity for energy and cost reduction.

Both quantities can be obtained either by calculation or by measurement, and the two routes are intrinsically linked. Calculation – from train-dynamics models, running-resistance formulations, and efficiency coefficients – is indispensable during design, feasibility assessment, timetable planning, and energy-storage sizing, when no physical system yet exists to measure [13, 14]. Measurement captures the energy actually consumed or recovered under real operating conditions and provides the ground truth against which calculation models are validated [10, 15]. Calculation models require measurements for their parameterization and validation (i.e., it is a fact that purely mathematical-physical equations will not yield accurate results due to inaccuracies and uncertainties), and measurement strategies presuppose an understanding of the physical and electrical processes the models represent; neither route is self-sufficient.

This duality is complicated by several factors recurring throughout the literature. Energy values depend strongly on where they are measured – at the onboard direct-current (DC) link, at energy-storage terminals, or at the substation – and on the temporal resolution of the instrumentation. The behavior of regenerative braking differs markedly between DC and alternating-current (AC) supply and between locomotive-hauled trains and distributed-traction electric multiple units (EMUs) [16]. Above all, the mechanically available braking energy becomes usable only to the extent that the surrounding network can accept it, a property known as receptivity. The absence of standardized definitions and reporting conventions across studies makes published figures difficult to compare and, in secondary syntheses, prone to misattribution. Figure 1 schematically sets out this operational energy balance.

The study will first identify available methods for calculating both traction energy types, then present corresponding measurement methods and compare them with respect to accuracy, required data, metering boundaries and applicability. In this context, the study will be particularly useful for design and for verifying energy savings on electrified railways, as both types of energy can be calculated and measured on the same basis.

The review is focused on four objectives. The first objective is to review design calculations for traction energy, acceleration energy and regenerative braking energy. This needs to be put into a suitable classification format. The second objective of the review is similar, but focuses on the measurement methods for traction energy, acceleration energy and regenerative braking energy.

The third objective of the review is to compare the design calculations and measurement methods on the basis of accuracy, required data, the metering boundary and applicability to different types of rolling stock (locomotives and EMUs) and to AC and DC systems. The last objective of the review is to achieve the best use of the energy a train can recover during braking. This review is confined to electric locomotives (of both heavy-haul and intercity passenger types) and EMUs (of both urban and regional types). These are supplied from AC or DC traction systems. Therefore, this review does not consider, for example, diesel-electric and hybrid locomotives, battery-only powered EMUs, and light-rail vehicles with a considerable amount of onboard energy storage. These types of rolling stock, however, contrast with the above-mentioned types.

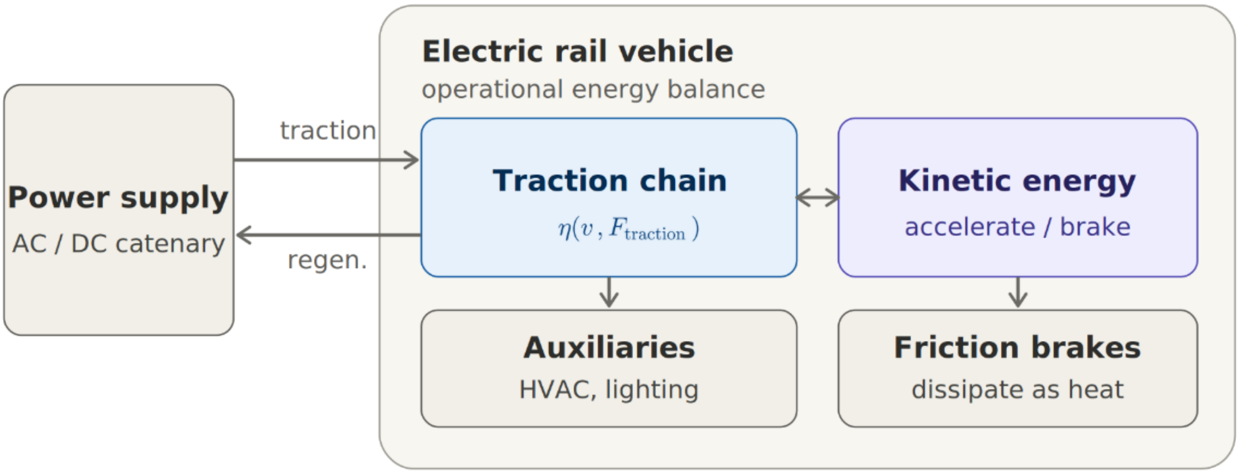

Fig. 1. Operational energy flow of an electric railway vehicle: traction (acceleration) energy supplied through the traction chain to the kinetic energy of the train and regenerated back during braking, with auxiliary demand and friction-brake dissipation as sinks (the explanation of the symbols can be found in Section 2.3)

The remainder of the paper is organized as follows: Section 2 sets out the review methodology, the classification framework, and the analytical foundations; Section 3 synthesizes and discusses the calculation and measurement options, together with the cross-cutting issues of receptivity, system type, and standardization; Section 4 draws conclusions and recommendations.

2. Methodology

This review: a synthesis of methods for the field, a classification framework for the vast field of research on this topic, and the set of governing equations used in the reviewed works to model trains and their behavior. This review is a synthesis of reviewed articles; i.e., no experiments were conducted to gather data for this review.

2.1 Literature Selection and Corpus

The scope of this review is not to design and perform a systematic literature search with a pre-registered search protocol, but to perform a structured review. Thus, the review is a critical review or a narrative review (also termed as 'narrative review' or 'review of reviews'). A total of 100 relevant publications from over 50 different authors and/or teams worldwide have been studied in this review. The relevant publications are mainly journal papers, conference papers and books, book chapters published by leading publishers worldwide. The reviewed publications have been grouped into two categories, i.e., the fundamental publications describing the basic principles of running resistance and energy-efficient operation [13, 17], and the recent research works and publications – published up to 2025, with a concentration in the 2019–2025 period – that describe the ways for energy-efficient railway transport. The results from a core of approximately 70 measurement-based studies (i.e., empirical studies) written by teams in Hungary and the surrounding region [10, 18] have formed the empirical 'backbone' of the results provided in this review. The results of these core studies, however, provide only an illustrative 'backbone' for the results reported in this review. In addition to the studies forming the core of this review, other studies employing different methodologies have also been included. The review reveals that the results for the acceleration energy presented here are based on a single, very large, high-quality measurement program conducted on selected railway lines operated by multiple operating teams, using a wide range of vehicles. Thus, there is a clear need to cross-validate the results reported in this review, both between operators and within an operator.

2.2 Classification Framework

The works were classified along a primary two-axis matrix and three cross-cutting axes. The primary matrix crosses the energy type – acceleration energy versus regenerative braking energy – with the analytical task – calculation versus measurement. The cross-cutting axes are: the supply system (AC versus DC), which determines the dominant physical constraint; the vehicle architecture (locomotive-hauled versus distributed-traction EMU), which affects efficiency and control response; and the metering boundary (onboard DC link, storage terminals, or substation), which determines what a reported figure actually represents. Within the calculation column, methods were further grouped as analytical (physics-based), simulation-based (multi-train, network-aware), and data-driven (statistical and machine-learning); within the measurement column, as onboard, wayside (substation), and hybrid. Figure 2 summarizes this classification, listing representative methods for each quadrant.

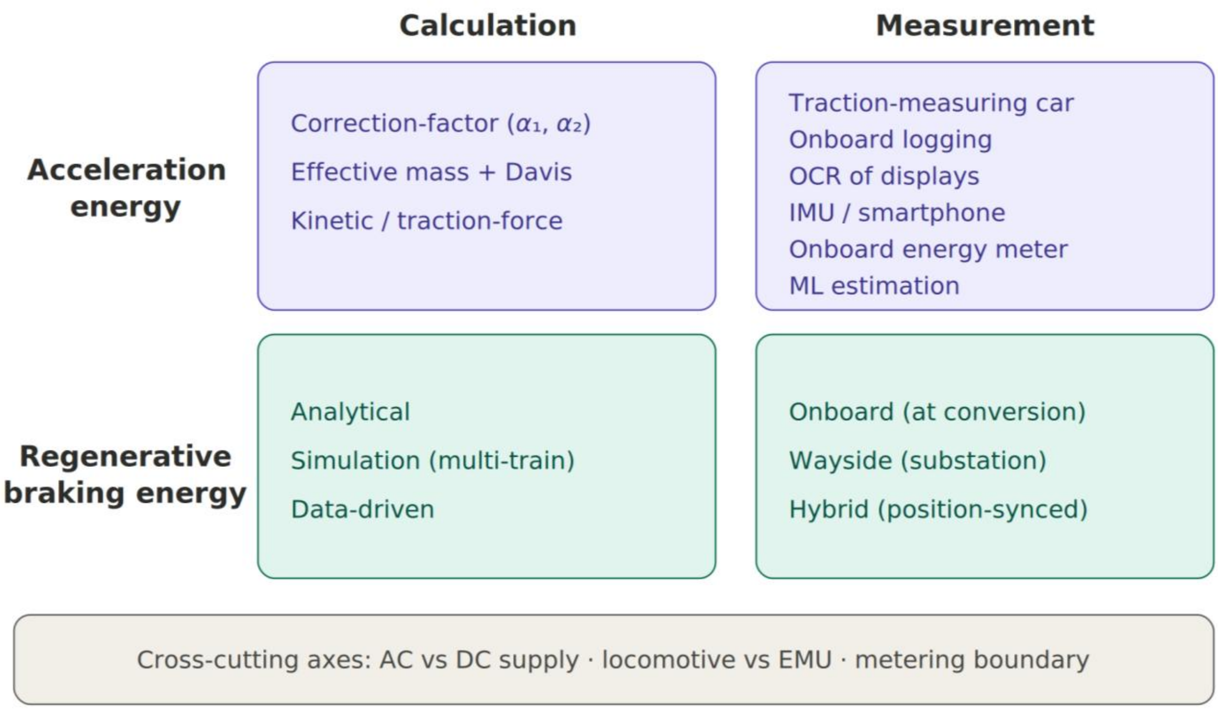

Fig. 2. Two-axis classification framework: energy type (acceleration versus regenerative braking) crossed with analytical task (calculation versus measurement), with the three cross-cutting axes. Representative methods are assigned to each quadrant (the explanation of the symbols can be found in Section 2.3)

2.3 Analytical Foundations

This subsection sets out the physical and mathematical basis used throughout the review. It introduces the effective mass and the running-resistance model (Section 2.3.1), the tractive-effort and acceleration-energy relations (Section 2.3.2), the multiplicative correction-factor method that links calculation to measurement (Section 2.3.3), and the decomposition of regenerative braking energy – used here interchangeably with the term recuperated braking energy adopted in the title – into available, recoverable, and utilized fractions (Section 2.3.4). The mechanical forces that enter these relations – the weight and its along-track and normal components, the normal reaction, the tractive effort, and the running resistance – are collected in the free-body diagram of Figure 3.

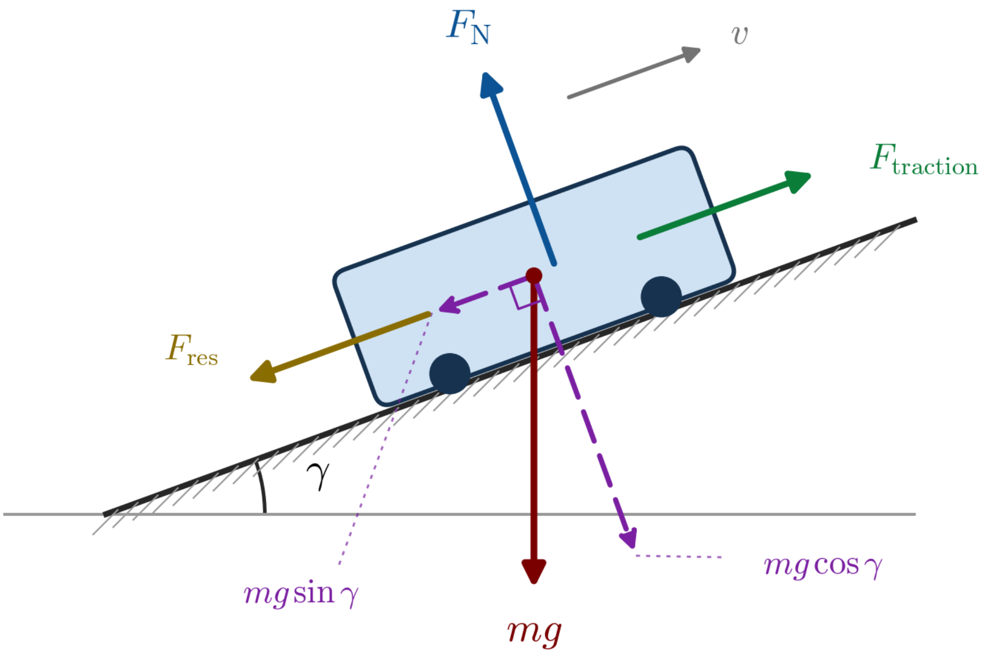

Fig. 3. Free-body diagram of a railway vehicle on a gradient, identifying the forces that enter the running-resistance, gradient, and tractive-effort relations of Section 2.3: the weight *mg* with its along-track component *mg* sin *γ* and normal component *mg* cos *γ*, the normal reaction F_N, the tractive effort $F_{traction}$, the running resistance F_{res}, and the ramp (track) inclination angle *γ*

2.3.1 Effective Mass and Running Resistance

A recurring source of error in simplified calculations is the use of the static train mass. Because wheelsets, gears, brake discs, and motor rotors must be accelerated angularly as well as translationally, the static mass *m* is replaced by an effective mass m_e (both in kg), given by Eq. (1), where the dimensionless rotational-inertia factor *ρ* typically lies in the range 0.06–0.15 for electric locomotives and 0.05–0.10 for EMUs; neglecting it underestimates the acceleration energy by roughly 6–15% [19, 20].

$$m_e = m \cdot (1 + \rho) \tag{1}$$

The motion resistance is almost universally represented by the Davis equation, Eq. (2), in which *A* captures speed-independent mechanical resistance, *B* the linear (flange-friction and turbulence) term, and *C* the quadratic aerodynamic-drag term (so that *A* is in N, *B* in N·s/m and *C* in N·s²/m²), with vehicle-specific coefficients markedly higher for locomotive-hauled trains than for streamlined EMUs; here F_{res} is the motion (running) resistance (in N) and *v* the running speed (in m/s) [13, 14, 21].

$$F_{res} = A + B \cdot v + C \cdot v^2 \tag{2}$$

Curve and gradient resistances are added as required; for a gradient e, the gradient term is $F_{grade} \approx m \cdot g \cdot e$, where g is the gravitational acceleration ($\approx$ 9.81 m/s²), and the gradient e is taken as a dimensionless rise-over-run ratio, so that F_{grade} results in N. For Hungarian passenger trains, the specific running resistance used in the reference studies is given by Eq. (3), in N/kN, with a separate formulation for freight trains [10]. In Eq. (3), v is in m/s, and the factor 3.6 converts it to km/h, while the numerical coefficients are empirical values fitted to the reference data.

Remark: Eq. (3) illustrates a vehicle-specific low/medium-speed empirical fit from [10], distinct from the full Davis form of Eq. (2).

$$\mu_{train} = 2.0 + 0.047 \cdot 3.6 \cdot v/100 \tag{3}$$

2.3.2 Tractive Effort and Acceleration Energy

The tractive force required at the wheel rim is the sum of the acceleration, resistance, and gradient components, $F_{traction} = F_{acc} + F_{res} + F_{grade}$, with $F_{acc} = m_e \cdot a$, where a is the acceleration (in m/s²). The electrical energy drawn from the supply follows from integrating the instantaneous power, $P_{el} = F_{traction} \cdot v \,/\, \eta$, over the acceleration interval (time t), as in Eq. (4); the resulting acceleration energy is E_{acc}, and the traction-chain efficiency η is itself a function of speed and load, $\eta = \mathrm{f}(v, F)$, and is suboptimal at start-up owing to winding and converter losses [22–25].

$$E_{acc} = \int (m_e \cdot a + A + B \cdot v + C \cdot v^2 + m \cdot g \cdot e) \cdot v \,/\, \eta(v)\, \mathrm{d}t \tag{4}$$

Two calculation routes are used in practice and were cross-validated in the present corpus: a kinetic-energy route, in which the acceleration energy is obtained from the change in kinetic energy of the effective train mass, and a traction-force route, in which it is obtained by integrating the measured or modeled tractive-effort curve over distance [18, 26]. These two routes use the same modeling basis as independent reviews of energy-efficient train control [27]. Independent studies confirm that the energy attributable to motion resistance is a sizeable, speed- and track-dependent share of the total, so that its accurate representation is decisive for both routes [28, 29].

2.3.3 The Correction-factor Method

A practical bridge between calculated and measured acceleration energy is the multiplicative correction factor α, defined by Eq. (5) so that the measured energy equals the calculated energy scaled by α, with separate factors α_1 for the kinetic-energy route and α_2 for the traction-force route [10, 18]. The factor accounts for the aggregate effect of conversion losses, auxiliary draw during acceleration, and modeling simplifications, and is determined empirically by regressing measured values against calculated values. In Eq. (5), E_{meas} is the measured acceleration energy, while $E_{calc,me}$ and $E_{calc,tf}$ are the calculated energies obtained via the kinetic-energy and traction-force routes, respectively.

$$E_{meas} = \alpha_1 \cdot E_{calc,me} = \alpha_2 \cdot E_{calc,tf} \tag{5}$$

2.3.4 Regenerative Energy: Available, Recoverable, and Utilized

For braking, the mechanically available energy over a deceleration from v_1 to v_2 is given by Eq. (6), where ρ is the rotational-inertia factor (see Eq. (1)) and Δh the net altitude change (positive for descending gradients, where gravity assists braking), with s the distance travelled during braking; the portion of this energy not recovered electrically is dissipated in the friction brakes, whose loading and wear are themselves the subject of dedicated study [30].

$$E_{available} = \tfrac{1}{2}\cdot m\cdot(1+\rho)\cdot(v_1^2 - v_2^2) + m\cdot g\cdot \Delta h - \int F_{res}(s)\,\mathrm{d}s \tag{6}$$

The recoverable electrical energy returned to the network is obtained by applying the efficiency chain of Eq. (7), with component efficiencies reported to be a few percentage points higher for EMUs than for locomotives. Here, η_{motor}, $\eta_{inverter}$, $\eta_{transmission}$ and η_{grid} are the efficiencies of the traction motor, the inverter (converter), the mechanical transmission, and the grid (line-side) interface, respectively.

$$E_{reg} = E_{available} \cdot \eta_{motor} \cdot \eta_{inverter} \cdot \eta_{transmission} \cdot \eta_{grid} \tag{7}$$

The recovery efficiency is then defined by Eq. (8), and its value depends critically on the metering boundary used to count the recovered energy. A central conceptual point is that available, recoverable, and utilized energy are three distinct quantities: the last is bounded by network receptivity, rather than by the train alone [31–33]. In Eq. (8), $E_{recovered}$ is the electrical energy actually returned through the chosen metering boundary and $E_{available}$ the mechanically available braking energy (as defined in Eq. (6)).

$$\eta_{recovery} = E_{recovered} / E_{available} \tag{8}$$

2.4 Measurement and Calculation Methods Considered

For acceleration energy, the corpus exercises a range of techniques: dedicated traction-measuring cars with calibrated instrumentation; onboard logging from the traction control system or onboard computer; optical character recognition (OCR) applied to recordings of onboard displays where direct data access is unavailable; inertial measurement units (IMUs), including smartphone sensors; onboard energy meters; and data-driven estimation from operational records. For regenerative braking energy, three approaches are distinguished: onboard measurement at the point of conversion; wayside (substation) measurement of the energy actually returned to the network; and hybrid, position-synchronized measurement combining the two. Calculation methods are grouped as analytical (fast, low-data, suitable for feasibility estimates), simulation-based (time-domain, multi-train, network-aware, suitable for timetable optimization and storage sizing), and data-driven (requiring large training datasets).

This review is not an experimental study; therefore, the claims are evaluated using triangulation. The quantitative information from the measurement-based studies is read in full and incorporated into this review in full. Information regarding graphs and numbers that have only been cited in secondary sources or by a single author within the reviewed literature is reported exactly as they have been presented in the cited work. This ensures that the reader is presented with the same context and uncertainty as in the cited work. If there is disagreement in the literature, the resulting ranges are presented. Most of the discrepancies between apparently similar numbers can be attributed to differences in metering boundaries and/or measurement resolution.

2.5 Nomenclature

The symbols used in Eqs. (1)–(9), and throughout the analytical foundations are listed in Table 1 below.

Table 1
Nomenclature: symbols, descriptions, and units used in the analytical foundations and Eqs. (1)–(9).

Symbol	Definition (unit)
A, B, C	Davis running-resistance coefficients (N; N·s/m; N·s²/m²)
a	Acceleration (m/s²)
E_{acc}	Acceleration energy (J)
$E_{available}$	Mechanically available braking energy (J)
$E_{calc,me}$, $E_{calc,tf}$	Calculated energy via the kinetic-energy and traction-force routes (J)
$E_{calc,me,rm,lift}$	Modified calculated acceleration energy (kWh)
E_{meas}	Measured acceleration energy (J)
$E_{recovered}$	Energy actually returned through the metering boundary (J)
E_{reg}	Recoverable regenerative energy (J)
e	Longitudinal track gradient, dimensionless rise-over-run ratio (-)
F_{acc}	Acceleration (inertial) force, $m_e \cdot a$ (N)
F_{grade}	Gradient resistance force (N)
F_N	Normal (support) reaction force (N)
F_{res}	Motion (running) resistance (N)
$F_{traction}$	Tractive effort at the wheel rim (N)
g	Gravitational acceleration (≈ 9.81 m/s²)
m	Train (static) mass (kg)
m_e	Effective mass, $m_e = m(1 + \rho)$ (kg)
P_{el}	Electrical power drawn from the traction supply (W)
s	Distance traveled (m)
s_{lift}	Along-track distance over which the gradient acts (m)
t	Time (s)
v	Running speed (m/s)
v_1, v_2	Initial and final speed of an acceleration or a deceleration (m/s)
v_j, v_{j+1}	Speeds at successive samples j and j+1 (m/s)
α, α_1, α_2, α_1*	Multiplicative correction factors (kinetic-energy / traction-force routes) (-)
γ	Track (ramp) inclination angle, $e \approx \tan\gamma \approx \sin\gamma$ (rad)
Δh	Net altitude change, $\lvert\Delta h\rvert = e \cdot s$ (m)
η	Traction-chain efficiency, $\eta = f(v, F_{traction})$ (-)
η_{motor}, $\eta_{inverter}$, $\eta_{transmission}$, η_{grid}	Component efficiencies of the regenerative chain (-)
$\eta_{recovery}$	Recovery efficiency (-)
μ_{train}	Specific running resistance (N/kN)
ξ_{rot}	Rotary-inertia (effective-mass) factor, 1 + ρ (-)
ρ	Rotational-inertia factor (-)

3. Results and Discussion

The evidence reviewed for the two investigated quantities, the sequence of calculation and measurement for acceleration energy (3.1 and 3.2) and for regenerative braking energy (3.3 and 3.4), is discussed subsequently. This is followed by a discussion of the evidence regarding the binding role of receptivity (3.5), AC/DC (3.6), locomotives and EMUs (3.6), and standardization and comparability (3.7). Finally, the evidence is compared, and suggestions are made regarding the choice of methods (3.8).

3.1 Acceleration Energy: Calculation

In the already well-established calculations for the energy spent by a train in its acceleration, a correction factor or several of them will be presented. The author of this paper measured these correction factors with the traction-measuring car of the Hungarian Railway Engineering and Metrological Service Center (REMSC) on the Öttevény-Hegyeshalom section of the railway line. The author measured the so-called correction factors for the V43 (older) and V63 (older) locomotives, several Siemens Taurus locomotives (1047), and a Stadler Flirt EMU. The author measured the aforementioned section at constant train speeds between 40 km/h and 160 km/h and during simulated post-restriction acceleration with a set brake force. The author will present the so-called correction factors they measured for the different train types and the older V43 and V63 locomotives (40–46% below their theoretical values), citing degraded rectifiers and non-original components. The correction factors are therefore, as the author already mentioned in their paper, empirical quantities, and their values can vary because the components of a vehicle are in different in-service conditions.

The same routes have recently been used for calculating the energy produced by Siemens Taurus (0470 series) trains on the Sopron-Győr line. The correction factors α_1 = 1.2981 and α_2 = 1.3151, with a coefficient of determination of above 0.99 for the filtered data, are 2.5–8.3% below the corresponding 2015 values of α_2 (1.331 and 1.415). This decrease is due to two main facts: on the one hand, the higher accuracy and resolution of the recent data; on the other hand, the train weights are no longer calculated from braking forces. The specific energy for constant-speed traction at 120 km/h is 0.00204 kWh/kN·km. The method is very stable, but the results are very sensitive to the input data, which must therefore be of very high quality. The values, calculated using the correction factors in Table 2, are accurate enough and even traceable.

Table 2
Correction factors α for acceleration energy of selected traction units (compiled from [10, 18])

Traction unit/train	Route/source	Factor (route)	Value
Taurus 0470, intercity	Sopron-Győr [18]	α_1 (kinetic energy)	1.2981
Taurus 0470, intercity	Sopron-Győr [18]	α_2 (traction force)	1.3151
Taurus, passenger	REMSC [10]	α (measured)	1.331
Taurus, freight	REMSC [10]	α (measured)	1.549
Stadler Flirt EMU	REMSC [10]	α (measured)	1.257
V43, passenger (aged stock)	REMSC [10]	α (measured)	2.121
V63, passenger	REMSC [10]	α (measured)	1.330

A further refinement comes from the most recent extension of this line of work, which enlarges the OCR-based dataset to 23 measurement runs and 391 filtered straight-section acceleration events recorded between November 2024 and September 2025 across six relations (Sopron-Győr, Sopron-Kelenföld, Kelenföld-Sopron, Sopron-Keleti, Kelenföld-Csorna, and Parndorf-Keleti), with Siemens Taurus 0470-, 0471-, 6182- and 1116-series locomotives (including one Railjet service) hauling intercity consists of 241–481 t (reported in a forthcoming companion conference paper by the present author [34]). Crucially, that companion study introduces a modified calculated acceleration energy that, unlike the earlier pure-mass formulation, incorporates both the rotational mass through a rotary-inertia factor ξ_{rot} = 1+ρ = 1.06 and the longitudinal-gradient lifting term, as in Eq. (9), and defines a corresponding correction parameter α_1* by $E_{meas} = \alpha_1{*}\cdot E_{calc,me,rm,lift}$. Because the earlier factors α, α_1 and α_2 [10, 18] were computed for pure masses on a flat track, they are made commensurable with α_1* simply by dividing by the 1.06 rotary-inertia factor, which clarifies that the various published factors describe the same underlying physics under different mass and gradient conventions.

$$E_{calc,me,rm,lift} = [\ 0.5 \cdot \xi_{rot} \cdot m \cdot (v_{j+1}{}^2 - v_j{}^2) \ \pm e \cdot m \cdot g \cdot s_{lift}\ ] \,/\, (3.6 \cdot 10^6) \tag{9}$$

In Eq. (9), $E_{calc,me,rm,lift}$ is the modified calculated acceleration energy (kinetic-energy route, including rotational mass and gradient lifting); v_j and v_{j+1} are the train speeds (in m/s) at successive samples j and j+1; ξ_{rot} = 1 + ρ = 1.06 is the rotary-inertia (effective-mass) factor (ρ = 0.06 was considered); m is the train mass (in kg); g is the gravitational acceleration (≈ 9.81 m/s²); e is the longitudinal track gradient (the dimensionless rise-over-run ratio, as in Eq. (4)) and s_{lift} the along-track distance over which it acts, its product $e\cdot s_{lift}$ being equal in magnitude to the net height change Δh of Eq. (6); so that the term ± $e\cdot m\cdot g\cdot s_{lift}$ is the potential-energy (lifting) contribution. The factor $3.6 \cdot 10^6$ converts joules to kWh, whereas Eqs (4) and (6) are expressed in SI units (joules).

Remark: the value ξ_{rot} = 1 + ρ = 1.06 corresponds to the complete locomotive-hauled InterCity consist rather than to the locomotive in isolation: the unpowered trailing coaches contribute only the small rotational inertia of their running gear yet account for most of the train mass, so the mass-weighted rotary-inertia factor of the whole train falls to the lower end of the per-locomotive range ρ = 0.06–0.15 given in Section 2.3.1.

Complementary calculation refinements in the corpus include the explicit treatment of effective mass and speed-dependent efficiency, as discussed in Section 2.3; the demonstration that mass reduction yields near-proportional acceleration-energy savings for stop-start services [35]; and the incorporation of dynamic traction-system efficiency into energy-efficient train control [22].

Underlying these correction-factor refinements are two complementary analytical routes to the acceleration energy itself. The first is the kinetic-energy route, in which the work delivered to the train is obtained from the change in translational kinetic energy scaled by the rotational-mass (effective-mass) factor of Section 2.3, with gradient and curve work added separately; it is transparent and well suited to rapid feasibility estimates. The second is the tractive-effort-integral route, in which traction energy is computed by integrating the resolved tractive effort over distance along the speed profile, the motion being governed by the balance between tractive effort, the Davis running resistance, and the gradient and curvature forces [13, 17]. The two routes agree only insofar as the running-resistance characterization is accurate: the Davis coefficients are sensitive to vehicle cross-section, surface, and formation length, and full-scale coast-down and tractive-effort tests remain the reference method for their determination [14]. Because uncertainty in these coefficients and in the effective-mass factor propagates directly into the calculated acceleration energy, measured correction factors – the Hungarian measurement series being one consistent example of an approach equally applicable to other fleets and networks – are precisely what is needed to reconcile calculation with practice, which is why the calculation and measurement strands of this review are inseparable.

Although the correction-factor values summarized above derive principally from one measurement program, their magnitude and behavior are consistent with the broader, independent evidence base. Independent energy-consumption models calibrated and validated against real electric-train data report a comparable few-percent reconciliation between calculated and measured traction energy once running resistance and conversion efficiency are properly represented [28].

Independent high-speed-train analyses confirm that motion-resistance energy is large and strongly speed-dependent [29] – the same sensitivity that renders the Hungarian factors condition-dependent. At the system level, independent work attributes roughly 70–75% of urban-rail electricity to traction and places the achievable savings from combined vehicle, operational, and infrastructure measures at about 25–35% [36], a context in which the few-percent reconciliation provided by the correction factor is best read as a calibration step rather than a savings measure. Crucially, the kinematic ingredients on which the calculation rests – the effective-mass factor and the Davis running-resistance coefficients – are themselves independently established [13, 19, 20], so that the principal vehicle- and network-specific quantity that measurement is needed to determine is the aggregate conversion efficiency rather than the kinematic terms.

3.2 Acceleration Energy: Measurement

The measurement of acceleration energy in the corpus spans a clear progression in instrumentation and cost. The dedicated traction-measuring car offers the highest fidelity, recording voltage, current, power, traction force at the drawbar, and synchronized speed and distance. Still, it is specialized, intrusive, and unsuited to routine fleet monitoring [10]. Onboard logging from the traction control system or onboard computer is less intrusive and supports diagnostics, and where direct data access is unavailable, OCR applied to high-frame-rate recordings of the onboard display – downsampled to 1 Hz – has been used to reconstruct consumed and regenerated energy, traction force, and catenary voltage for Taurus 0470 trains [18]. The same study notes a hardware-dependent limitation: locomotives whose onboard computers refresh only every twenty seconds or so (e.g., some Vectron units) are unsuited to fine-grained analysis, whereas the Taurus display permitted 1 Hz reconstruction. Beyond direct metering, data-driven estimation offers a complementary low-cost route: machine-learning models trained on basic kinematic features – train speed, acceleration, track gradient, and curvature radius – have reproduced the traction power of a metropolitan line with good accuracy, reducing reliance on costly instrumented runs [37].

At coarser resolution, bulk telemetry has been exploited for fleet-scale statistical analysis: five-minute-resolution onboard records for distributed-traction EMUs were processed with geodesic distance reconstruction, interquartile-range outlier filtering, and polynomial curve fitting to model route- and month-specific consumption and to localize over-consumption hotspots. Such datasets are candid about the limits of coarse, anonymized data: individual accelerations, instantaneous speeds, and driver identities could not be resolved, thereby precluding driver-level analysis. Independent measurement-based modeling reaches a similar verdict on what onboard data can resolve. Once auxiliary demand and conversion efficiency are accounted for, metered traction energy matches physics-based estimates to within a few percent, while residual variance tied to driver behavior and operating conditions persists across fleets [28]. Lower-cost approaches include IMU- and smartphone-based acceleration measurement, attractive for their accessibility but limited by vibration, drift, and the absence of railway-grade calibration [38, 39], and onboard energy meters fitted to heavy-haul trains for continuous efficiency monitoring [15]. Data-driven estimation – from data mining of operational factors [40] to machine-learning prediction of traction energy [41–43] – increasingly supplements direct measurement when large datasets are available. Across these options there is a clear fidelity–cost gradient – from high-fidelity but specialized, intrusive traction-measuring cars and onboard energy meters, through onboard computer logging and OCR of cab displays that are limited by refresh rate and legibility, to the low-cost but event-blind and uncalibrated bulk-telemetry and IMU/smartphone approaches – with data-driven estimation accurate only where large, clean datasets exist; these correspond to the measurement column of the acceleration row in Figure 2.

A distinctive use of measurement is diagnostic. By comparing measured against calculated acceleration energy, the residual can be interpreted as system loss: a measured value substantially above the calculated baseline signals converter, winding, transmission, or running-resistance degradation, converting energy measurement from passive accounting into an active condition-monitoring tool [44].

3.3 Regenerative Braking Energy: Calculation

Analytical calculation of regenerative energy is based on the available-energy model of Section 2.3 and the efficiency chain. Physics-based models that incorporate continuous gradient profiles, speed-dependent adhesion limits, and motor-characteristic curves have reproduced measured recovery on long downhill EMU sections to within about ±8% in the reviewed corpus, with the accuracy attributed to the use of real motor-efficiency maps rather than constant-efficiency assumptions. For DC systems, models that explicitly simulate the control response to rising line voltage capture the threshold at which regenerative braking is progressively curtailed and replaced by rheostatic braking – a critical feature, since voltage rise rather than mechanical capacity is the primary DC constraint [45].

Simulation-based methods become necessary in multi-train settings, where energy from a braking train may be consumed by another accelerating train before reaching a substation. Time-domain models of AC and DC supply networks, incorporating substation and rectifier models, line impedance, and timetable-driven train demand, show that local consumption can substantially reduce substation-exported regenerative energy relative to a single-train idealization [31]. The practical implication is that storage sizing based on single-train calculations is liable to be oversized. Data-driven calculation forms a third route: neural-network models trained on large sets of braking events have predicted per-event regenerative energy with mean absolute percentage errors in the high single digits, comparable to or slightly better than analytical baselines on the same data, but contingent on large, clean, regularly retrained datasets [41, 46]. The three calculation families trade data requirements against accuracy: physics-based analytical methods need minimal inputs and suit feasibility estimates (indicatively within about ±15%); multi-train, network-aware simulation requires the timetable and supply model but tightens agreement to roughly ±5–10% and is appropriate for timetable and storage sizing; and data-driven prediction reaches mean absolute percentage errors in the high single digits to low teens where large, clean event datasets exist. These accuracy bands are indicative and method-dependent rather than fixed constants, since they originate in single studies under specific assumptions; the three families correspond to the calculation column of the regenerative row in Figure 2.

3.4 Regenerative Braking Energy: Measurement

Onboard measurement captures regenerated energy at the point of conversion between the traction converter and the train's electrical system. It is the most direct route, but it requires installed instrumentation and careful synchronization with position data to attribute energy to track sections [12]. Wayside measurement, using bidirectional meters at substation feeders, captures only the energy that actually returns to the network; on DC systems, a large fraction of onboard-measured regenerated energy is consumed locally by other trains or lost in line resistance before reaching a substation, so wayside measurement alone systematically underestimates recovery, with the discrepancy larger at lower system voltages. Hybrid, position-synchronized measurement combining onboard and substation meters is therefore the reference approach for validation studies, at the cost of complexity and expense, which confine it to representative test trains and substations [31, 47].

A consistent theme is the dominance of the sampling rate. Averaging over multi-second intervals – let alone the multi-minute aggregation of standard utility meters – misses short-duration regenerative transients and underestimates energy recovery; the reviewed sources recommend high-frequency sampling at hundreds of hertz to 1 kHz for event-level accuracy. These figures are reported in secondary form in the corpus and should be verified against the primary instrumentation studies before being cited as design thresholds.

Measurement series on Hungarian and neighboring lines provide concrete measured values. On the Hegyeshalom-Győr section, Railjet measurement series have indicated that regenerative braking energy can reach roughly 20–30% of the consumed energy, with a wide best-to-worst spread largely attributed to driving style and the placement of speed restrictions. On the Raaberbahn network, route- and month-resolved regenerative energy for distributed-traction EMUs has shown direction- and terrain-dependent patterns, with one direction generating more regenerative energy than the other on the same line. For Taurus 0470 trains on the Sopron-Győr line, heatmaps localized both consumption and regenerative braking energy around stations and turnouts, consistent with the concentration of acceleration and deceleration near those locations [18]. The last study also noted an important contrast in utilization: the Taurus electric braking force is limited to about 150 kN, whereas Vectron locomotives can provide roughly double that, so vehicle choice directly affects recoverable energy. Comparable quantification beyond the Hungarian network is reported for high-stop-frequency light-rail operation, where the regenerative energy recovered as a share of consumption was found to differ measurably between the two running directions of the Addis Ababa Light Rail Transit [48], corroborating the directional asymmetry observed on the Raaberbahn EMU services.

3.5 Utilization and Receptivity: the Binding Constraint

The recurring conclusion across the regenerative-energy literature is that the limiting quantity is not the mechanically available energy but the network's capacity to absorb it. Three mechanisms govern utilization. The first is train-to-train transfer within a power section, whose effectiveness depends on the temporal overlap between a braking train and a nearby accelerating one – and hence on timetable structure and dwell control [33, 49]. The second is export to the upstream grid through reversible or inverter substations, which provide a stable recovery path where local demand is insufficient and which avoid overvoltage by diverting excess energy when the DC line voltage exceeds a threshold [32, 50]. The third is storage, in onboard or wayside energy-storage systems whose technology is matched to the load spectrum: supercapacitors and flywheels for the frequent, short pulses of urban DC metros, and hybrid energy-storage systems (HESS) combining batteries and supercapacitors for the mixed time-scales of high-speed and main-line service [51–58]. The choice between onboard and wayside placement of such storage, and its sizing against the regenerative load spectrum, has been examined since early kinematic and network-simulation studies [59, 60], which established that stationary supercapacitor banks at substations and onboard devices capture complementary fractions of the recoverable energy on low-voltage DC metro lines; subsequent work has sharpened the technology choice – flywheels versus supercapacitors for wayside duty [61] – and the joint optimisation of sizing and scheduling for hybrid storage at AC traction substations [62]. Figure 4 summarises this picture, tracing the cascade from available to recoverable to utilized energy, together with the mechanisms and constraints that govern it.

Comparative studies place these three receptivity mechanisms side by side rather than treating them in isolation. A comprehensive review classifies recuperation techniques into uncontrolled and controlled schemes spanning onboard and wayside energy storage, reversible (inverter) substations, and their combinations, and offers selection guidance keyed to system voltage, traffic density, and line layout [63]. A more recent comprehensive review focused specifically on railway energy-storage systems reaches the same conclusion from the storage side, surveying onboard, wayside, and hybrid configurations, along with their sizing and control, and confirming that the technology choice is governed by line- and traffic-specific receptivity rather than by storage performance alone [64]. Quasi-static network simulations that place onboard storage, wayside storage, and reversible substations into the same set of realistic operating scenarios confirm that no single technology dominates: the most effective choice depends on substation spacing, traffic density, and the degree of natural train-to-train exchange already present [65]. Coordinating devices is consistently better than deploying them singly – jointly optimized control of reversible substations together with wayside storage improves both line-voltage stabilization and net energy savings on metro networks beyond what either achieves alone [66] – which, at the hardware level, restates the systemic nature of receptivity. At the device level, stationary supercapacitor banks sized per substation to absorb each station's regenerative-current peaks, with the storage rating fixed by the predicted instantaneous regenerative energy and the configuration justified by a benefit–cost analysis, have been dimensioned in exactly this way for an urban metro line [67]. The control layer that governs such storage is itself an active design variable: hybrid battery–supercapacitor schemes managed by fuzzy-logic supervisory controllers, demonstrated in the adjacent automotive regenerative-braking domain, show how the power split between high-energy and high-power elements can be regulated to protect the storage and maximize recovered energy, with principles that transfer directly to onboard rail storage [68]. Because no single recuperation technique dominates, the selection and coordination of these calculation methods, metering boundaries, and storage or substation options is increasingly framed as a multi-criteria decision problem and supported by formal decision-making and ranking methods [69].

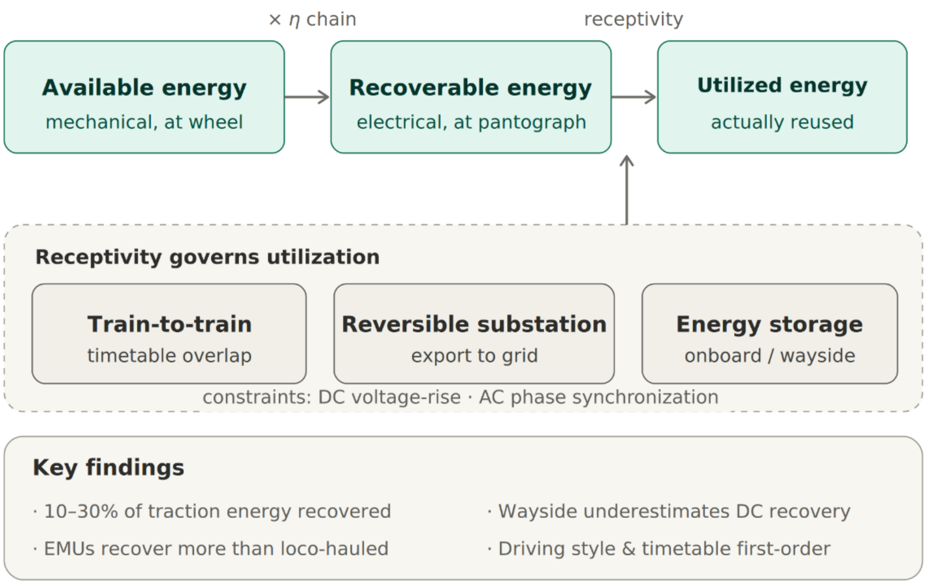

Fig. 4. From available through recoverable to utilized regenerative braking energy: the efficiency chain, the three receptivity mechanisms (train-to-train transfer, reversible substations, energy storage), their physical constraints, and the principal findings; on the basis of [11, 31–33, 49, 50, 51–58, 70, 71]

Two case studies in the corpus illustrate the contrast between operational and technological routes to higher receptivity. On a 750 V DC third-rail metro (Malaysian MRT Line 2, a 57.7 km driverless line), a traction-power simulation reported a net traction-energy reduction in excess of 50% in an optimised timetable scenario that maximises the overlap of braking and accelerating trains

– a result obtained under idealising assumptions (balanced three-phase supply, constant headway and dwell) and therefore best read as an optimistic upper bound [47]. More generally, multi-train trajectory optimization has been used to reshape the running-time allocation of an entire timetable so that the braking and accelerating phases of different trains coincide, raising the energy efficiency of a given schedule without additional hardware [70]. On a 1.5 kV DC metro (São Paulo Metro Line 1, 20.2 km), retrofitting rectifier substations with inverter substations was reported to recover on the order of 9–41% of substation energy depending on traffic density, with a representative substation-level reduction of about 13% and an investment payback well within the assumed service life [71]. These figures are drawn from the reviewed primaries; given their single-line, single-study basis, they should be cited with their assumptions and verified against the originals.

To make the dependence on metering boundary explicit, Table 3 collates representative reported regenerative-energy figures across systems together with the boundary and basis attached to each. Because those boundaries differ – train-level recovery, substation-level export, and net traction-energy reduction are distinct quantities – the entries should be read together with the final column rather than compared as if they were the same measure.

Table 3
Reported regenerative braking energy across selected systems, by metering boundary and basis

System (line)	Supply	Reported regenerative figure	Metric, boundary, and source
Cross-study range (urban and main-line)	AC and DC	≈10–30% of traction energy	Recovered share; range across studies [11, 12]
Railjet, Hegyeshalom-Győr	25 kV AC	≈20–30% of consumed energy	Onboard measurement; train level
Addis Ababa LRT	DC (light rail)	Direction-dependent share of consumption	Operational estimate; train level [48]
São Paulo Line 1	1.5 kV DC	≈9–41% (≈13% typical) of substation energy	Substation export via inverter substations [71]
Malaysian MRT Line 2	750 V DC	>50% net traction-energy reduction	Network simulation, optimized timetable; idealized upper bound [47]

3.6 Cross-cutting Distinctions: AC versus DC, Locomotive versus EMU

The dominant physical constraint differs by supply type. DC systems are constrained by voltage rise: on a 750 V system, the upper limit (commonly 900 V) can be reached within a second or two of brake application when no nearby train is drawing power, forcing a switch to rheostatic braking and explaining why measured DC recovery often falls short of theoretical calculations. AC systems are instead constrained by phase synchronization and power quality, but benefit from longer feeding sections and lower sensitivity to distance from the substation [31, 72]. On the DC side specifically, Popescu and Bitoleanu [73] comprehensively survey the available efficiency measures – substation reinforcement, reversible converters, and wayside storage – and their interactions with the voltage-rise limit. The asymmetry is structural: on 25 kV AC lines the four-quadrant (active front-end) converters of modern traction units return surplus energy through the transformer to the upstream grid almost as a by-product, whereas on 750 V and 1.5 kV DC lines the diode rectifiers of conventional substations block any return, so that DC recovery depends entirely on a receptive neighbouring train, a reversible substation, or wayside storage [65]. The principal contrasts are summarised in Table 4.

This structural asymmetry is made explicit in Figure 5. On 25 kV AC lines, the four-quadrant (active front-end) line converter of a modern traction unit is inherently bidirectional, so braking energy not absorbed onboard flows back through the main transformer to the upstream grid as a routine by-product of normal operation. On conventional DC lines, by contrast, the diode rectifiers of the feeding substation conduct in one direction only and cannot pass energy back to the grid; recovered energy must therefore reach one of three alternative sinks – a receptive neighboring train within the same supply section, a reversible (inverter-equipped) substation, or onboard or wayside storage – and is otherwise dissipated in the rheostatic brake. The same vehicle under identical driving conditions can thus report materially different recovered-energy figures on AC and DC infrastructure, which is why the DC limitation is properly regarded as structural rather than merely operational.

Table 4
AC versus DC traction systems: dominant constraints and characteristics

Parameter	DC (750/1500/3000 V)	AC (25 kV 50 Hz)
Primary constraint	Voltage rise [65, 73]	Phase synchronisation [31, 72]
Typical regen. efficiency	0.70–0.80 [31–33]	0.75–0.85 [31–33]
Wayside measurement	Lower (local consumption) [65, 73]	Higher (longer sections) [31, 72]
Sensitivity to distance	High (voltage drop) [73]	Low (high voltage) [31, 72]

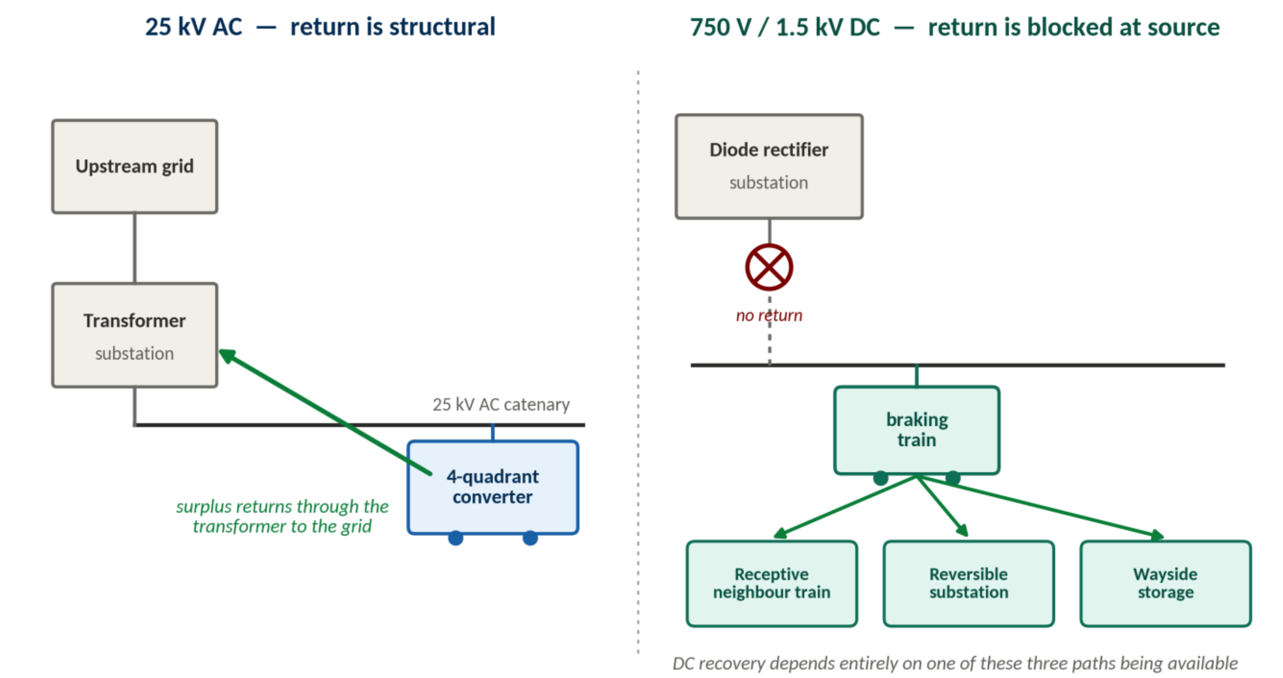

Fig. 5. Recovery-path asymmetry between AC and DC traction supply: on 25 kV AC lines the four-quadrant line converter returns surplus braking energy through the main transformer to the upstream grid as a routine by-product, whereas on 750 V/1.5 kV DC lines the diode rectifiers of conventional substations block any return, so that recovered energy must be taken up by a receptive neighbouring train, a reversible substation, or onboard/wayside storage (cf. Table 4)

Vehicle architecture also matters. Distributed-traction EMUs are reported to achieve higher regenerative efficiency than locomotive-hauled trains of comparable load – by something like 6–15 percentage points in the secondary sources – owing to multiple powered axles operating at favorable partial load, shorter motor-to-pantograph paths with lower line-resistance losses, and faster modern converter control. This qualitative ordering is consistent with the measured Hungarian context, in which EMU studies (Flirt, Ventus) and locomotive studies (Taurus, Railjet) were conducted within the same methodological family [10, 18]; the precise differential, however, is reported in secondary form and warrants primary verification.

Operational levers are consistently identified as the most cost-effective, with systems-level appraisals of urban-rail energy singling out operating strategy and regenerative braking as the largest opportunities for savings [36]. At the operations-planning level, energy-saving optimization of the speed profile and coasting points – solved with an improved brute-force search that explicitly credits recovered braking energy – has likewise been shown to reduce net traction energy for a metro service [74]. Driving style is repeatedly found to be a first-order determinant of both consumed and recovered energy [75], motivating driver-advisory systems (DAS) and automatic train operation (ATO) [76–78]. The optimal driving strategy that such systems implement is assembled from four canonical regimes – maximum traction, cruising, coasting, and braking – whose sequence and switching points follow from Pontryagin's maximum principle and from the running-time supplement carried in the timetable, as consolidated in the review of energy-efficient train control and timetabling by Scheepmaker *et al.* [27]. Timetable and speed-profile optimization can, in turn, substantially increase the utilization of regenerative energy without hardware investment [49, 79–86]. Reinforcement learning and metaheuristic control of speed profiles extend these gains [87–91].

These four regimes, and the way they govern the two target energies, are drawn together in Figure 6, which maps a representative inter-station speed profile onto the analytical foundations of Section 2.3. During the maximum-traction phase, the train draws the acceleration energy of Eqs. (4) and (9); during cruising and coasting, the tractive demand falls to the running-resistance level of Eq. (2) or to zero; and during braking the kinetic energy of the effective mass becomes mechanically available for recovery according to Eq. (6), of which only the fraction admitted by the efficiency chain of Eq. (7) and by network receptivity is ultimately returned. Setting the regimes out in this way makes clear that the acceleration-energy correction factor and the recovery efficiency act on different, non-overlapping phases of a single journey, and that the switching points between regimes – the decision variables of energy-efficient driving – are exactly what driver-advisory and automatic-train-operation systems adjust in order to shift energy from dissipation toward recovery.

The strongest direct evidence for the magnitude of the driving-style effect on the Hungarian network comes from disaggregating the acceleration-energy correction factor at the level of individual drivers, as set out in a forthcoming companion study by the present author [34]. Across the 391 events and 14 anonymized drivers in that forthcoming analysis, the measured-to-calculated energy ratio is not a driver-independent constant. For the four drivers represented by at least two runs, the per-event ratio medians of three drivers cluster between about 1.21 and 1.28, close to the global median of 1.241. In contrast, one driver exhibits a sub-unity median of roughly 0.77 – meaning that on a substantial fraction of his acceleration events, the measured electrical energy was actually smaller than the calculated kinetic increment. The deviation from a per-relation baseline is, moreover, directionally asymmetric: one driver differed by about +38% in one travel direction and −11% in the opposite direction on the same relation pair, pointing to an intra-driver, context-dependent component (gradient profile, station-approach strategy) on top of the inter-driver spread. The author notes that the magnitude of this driver-related variability is broadly comparable to that attributable to traction-component conversion losses, and that the per-event ratio is sensitive to small denominators near station departure; a quantitative follow-up using mixed-effects models with driver as a random factor is in preparation. These observations corroborate, for rail, the heavy-haul finding that driver behavior can be the single largest influence on specific energy consumption [15]. They reinforce the case for driver-advisory systems, targeted driver training on regenerative braking, and treating the human operator as an explicit covariate rather than as measurement noise in railway energy models [75]. This operator effect is consistent in magnitude with the road-transport literature, where controlled studies attribute an inter-driver coefficient of variation of roughly 10–23% in energy use and CO_2 emissions to driving style alone [92], and comparable behavioral metrics – such as an automatically extracted attention-horizon indicator that correlates with fuel consumption – have been proposed and could transfer to train drivers [93].

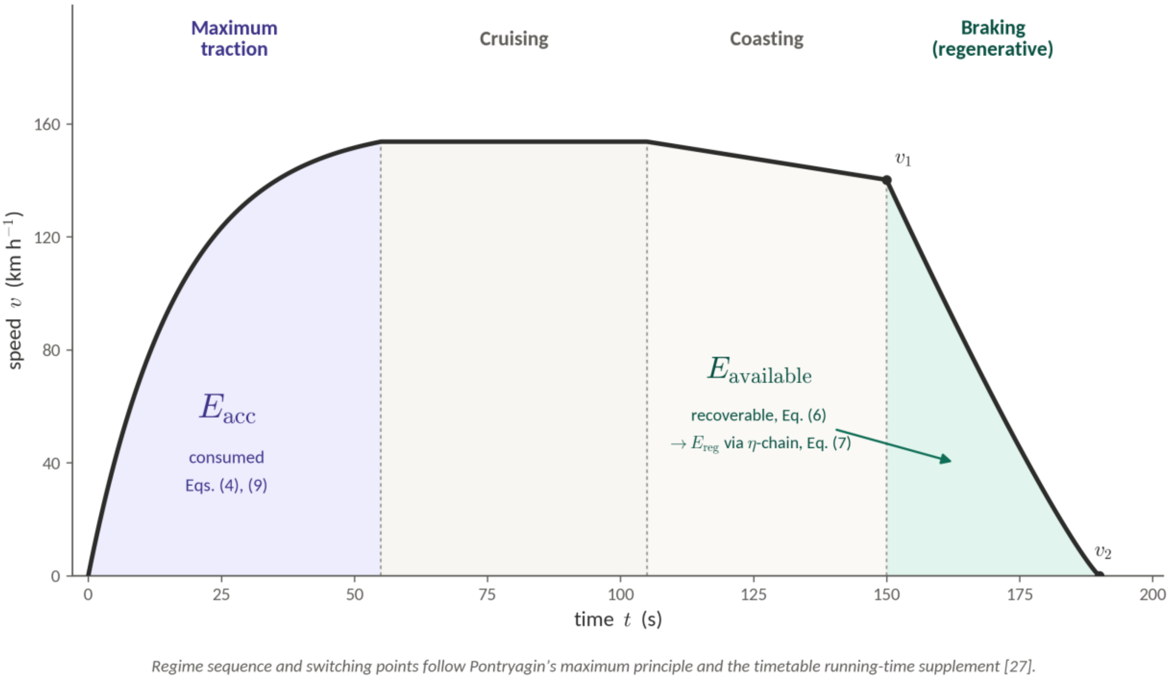

Fig. 6. Representative inter-station speed profile and the four canonical driving regimes (maximum traction, cruising, coasting, braking), showing where each energy quantity of Section 2.3 applies: the acceleration energy of Eqs. (4) and (9) during traction, and the mechanically available braking energy of Eq. (6) – recoverable through the efficiency chain of Eq. (7) – during braking. The regime sequence and switching points follow Pontryagin's maximum principle and the timetable running-time supplement [27]

3.7 Standards, Metric Inconsistency, and Comparability

The most serious obstacle to cumulative progress is methodological rather than technological. Studies report recovered energy, efficiency gains, voltage reductions, or economic savings, but use inconsistent boundaries and definitions, so headline figures are frequently not comparable. The European standards for onboard energy measurement and for traction power supply (the EN 50463 [94] series for energy measurement onboard rolling stock and EN 50388 [95] for power supply and rolling-stock coordination), and emerging common frameworks, are steps toward harmonization. The reviewed sources converge on a reporting-quality recommendation: any study presenting regenerative or acceleration energy should document the measurement location, sampling rate, instrument-accuracy class, train mass, gradient profile, efficiency assumptions, and uncertainty bounds, without which results cannot be reproduced or compared. The present review's own experience reinforces this point: several figures circulating in secondary syntheses could be traced to a single study under specific assumptions, and some had been misattributed across the literature, underscoring the need to cite the primary studies and to record the metering boundaries explicitly.

The most developed harmonization effort is the European standard for onboard energy measurement, EN 50463, which, since its first issue in 2007, has evolved through the 2012 and 2017 editions into a complete specification for an interoperable Energy Measurement System (EMS) [94]. The series is organized by function: a general part fixes terminology and architecture; an energy-measuring part specifies the voltage-measurement, current-measurement, and energy-calculation functions together with their accuracy classes; a data-handling part defines how the measured quantities are aggregated into compiled energy billing data; a communication part governs the transfer of those data to ground, for which it relies on the train communication network standard for on-board-to-ground links [96]; and a conformity-assessment part defines verification of a complete installation. For the present review, the decisive point is that EN 50463 fixes the metering boundary at the contact-line interface – the pantograph or current collector – and treats energy returned to the supply during regenerative braking as a signed quantity within the same accounting, so that consumed and recuperated energy are measured on one consistent, billable basis. Where studies report against this boundary, their figures are directly comparable; where they do not, the boundary must be stated before any comparison is meaningful.

Figure 7 positions this EN 50463 boundary relative to the alternatives encountered throughout the review. The same braking event is registered as a different quantity depending on where it is metered: at the pantograph or current collector – the EN 50463 [94] billing boundary, on which consumed and recuperated energy are counted as one signed, contact-line quantity; at the onboard DC link, the point of conversion, which captures energy before any network interaction; at the substation feeder, which sees only the fraction actually returned to the network and therefore systematically underestimates recovery on DC systems; or through an inertial proxy derived from kinematics, which estimates mechanical rather than electrical energy. Because these boundaries enclose physically distinct quantities, a reported figure becomes interpretable only once its boundary is stated, and the shares, efficiencies, and reductions collated in Tables 3 and 5 must each be read against the boundary attached to it – the single most consequential reporting convention for the comparability that this section calls for.

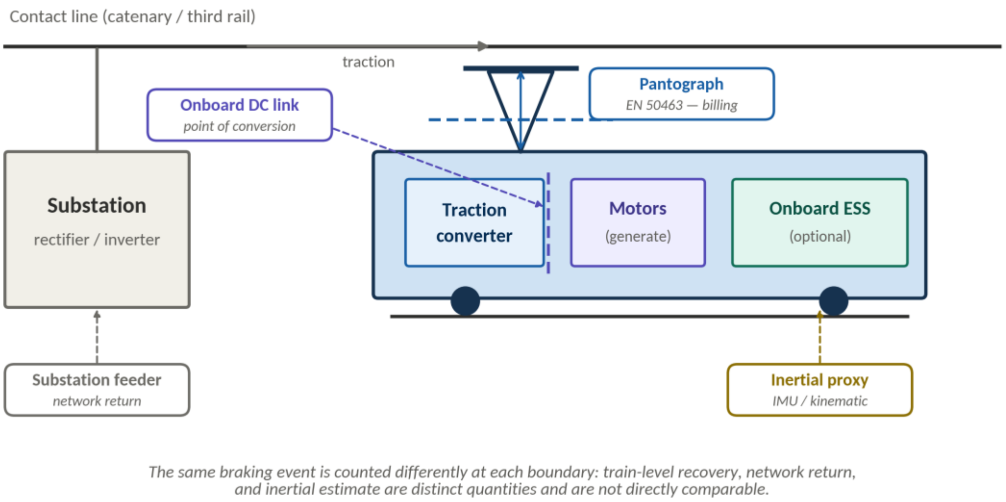

Fig. 7. Metering boundaries for railway traction energy and the quantity each one captures: the pantograph/contact-line interface (the EN 50463 [94] billing boundary), the onboard DC link (point of conversion), the substation feeder (network return, which underestimates recovery on DC systems), and an inertial/kinematic proxy (mechanical estimate). Reported energy figures are comparable only when read against the boundary attached to each (cf. Tables 3 and 5)

Two further standards close the loop between calculation and measurement. EN 50591 [97] specifies how the energy consumption of rolling stock is to be calculated through a defined simulation methodology and verified by measurement, thereby bridging the design-stage figures of Section 3.1 and the onboard metering of Section 3.2 [97]. EN 50388, in turn, sets the technical criteria for coordinating the traction power supply with the rolling stock, including the conditions under which regenerative braking may be injected into the network and the line-voltage limits that bound its acceptance – in standards language, the receptivity that Section 3.5 identifies as the binding constraint [95]. Read together, these instruments define a coherent chain: calculate consumption by a common method (EN 50591 [97]), measure it to a common boundary (EN 50463 [94]), and admit recuperated energy under common power-supply criteria (EN 50388 [95]). The persistence of non-comparable figures in the literature therefore reflects incomplete adoption of this chain rather than its absence, and convergence on it is the single most effective step the field could take toward cumulative, comparable results.

3.8 Comparative Synthesis and Method Selection

Table 5 consolidates the calculation and measurement options reviewed above and maps them to the decisions they best support, addressing objective (iii). Two practical rules emerge. First, the method should be chosen by the decision at hand rather than by data availability alone: analytical correction-factor estimates suffice for early feasibility, multi-train simulation is warranted for timetable and energy-storage decisions, and high-fidelity onboard or hybrid measurement is reserved for validation, billing, and receptivity studies. Second, every reported figure must travel with its metering boundary, because the same train can yield materially different values at the pantograph, at the substation, or through an inertial proxy.

Table 5
Comparative assessment of calculation and measurement methods and their decision contexts

Method	Energy type & task	Fidelity/data needs	Metering boundary	Best-suited decision context
Correction-factor / kinetic-energy & tractive-effort routes [10, 18, 26]	Acceleration calculation	Moderate; low data (mass, resistance, efficiency)	— (model)	Design, feasibility, rapid screening
Multi-train simulation [31, 59, 60, 70]	Both calculation	High at system level; needs network, timetable, ESS data	— (model)	Timetabling, ESS sizing, receptivity
Data-driven / machine learning [37, 40, 41–43, 46]	Both calculation	Variable; needs large, curated datasets	— (model)	Fleet-scale estimation, diagnostics
Dedicated traction-measuring car [10]	Acceleration measurement	Highest fidelity; high cost, intrusive	Pantograph/ drawbar	Reference & model validation
Onboard logging/ energy meters [15]	Acceleration & regen. measurement	High; moderate cost	Pantograph (onboard)	Operational monitoring, billing (EN 50463 [94])
OCR from onboard display [18, 34]	Acceleration measurement	Moderate; low cost, no direct data access	Onboard (indirect)	Retrospective estimation where data unavailable
IMU/smartphone sensors [38, 39]	Acceleration measurement	Low-moderate; very low cost, no rail-grade calibration	Vehicle motion (indirect)	Low-cost screening
Wayside/substation metering [32, 71, 73]	Regen. measurement	Underestimates recovery on DC	Substation	Network-return accounting
Hybrid position-synchronized [65, 94]	Regen. measurement	High; synchronized onboard + wayside	Onboard + substation	Receptivity & ESS-sizing decisions

The fidelity-cost trade-off among the measurement methods, described qualitatively in Section 3.2, is made explicit in Figure 8. The methods fall along a clear gradient: dedicated traction-measuring cars and position-synchronized hybrid set-ups deliver the highest fidelity at the greatest cost and intrusiveness; onboard energy meters and control-system logging occupy an attractive middle ground; and optical character recognition, inertial or smartphone sensors, and machine-learning estimation provide low-cost, lower-fidelity access where direct instrumentation is unavailable. Wayside (substation) metering sits below the frontier because, on DC systems, it records only the energy actually returned to the network, thereby understating train-level recovery. Reading the methods in this plane clarifies that the appropriate choice is the one that meets the fidelity a given decision requires at the lowest justifiable cost, rather than the most accurate method available in the abstract.

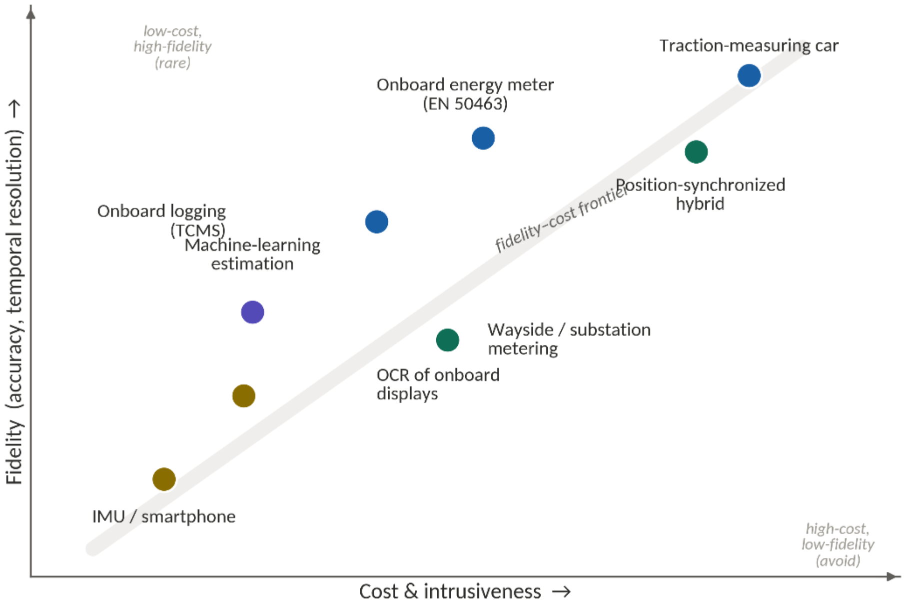

Fig. 8. Fidelity versus cost and intrusiveness of the railway energy measurement methods (Section 3.2). The methods trace a fidelity–cost frontier; wayside/substation metering sits below it because it captures only network-returned energy on DC systems. The plane positions each method for the selection guidance of Table 5

These selection principles are brought together in Figure 9, which turns Table 5 into an actionable decision aid. Starting from the decision to be supported, it routes early-feasibility screening to the analytical correction-factor method; timetable and energy-storage sizing to multi-train network simulation; validation, diagnostics, and billing to high-fidelity onboard measurement referenced to the EN 50463 [94] boundary; and receptivity or network-return studies to position-synchronized hybrid measurement. Each branch has its own characteristic data requirements and metering boundary, and the figure restates the two governing rules: choose the method based on the decision rather than on data availability, and report each figure with its metering boundary.

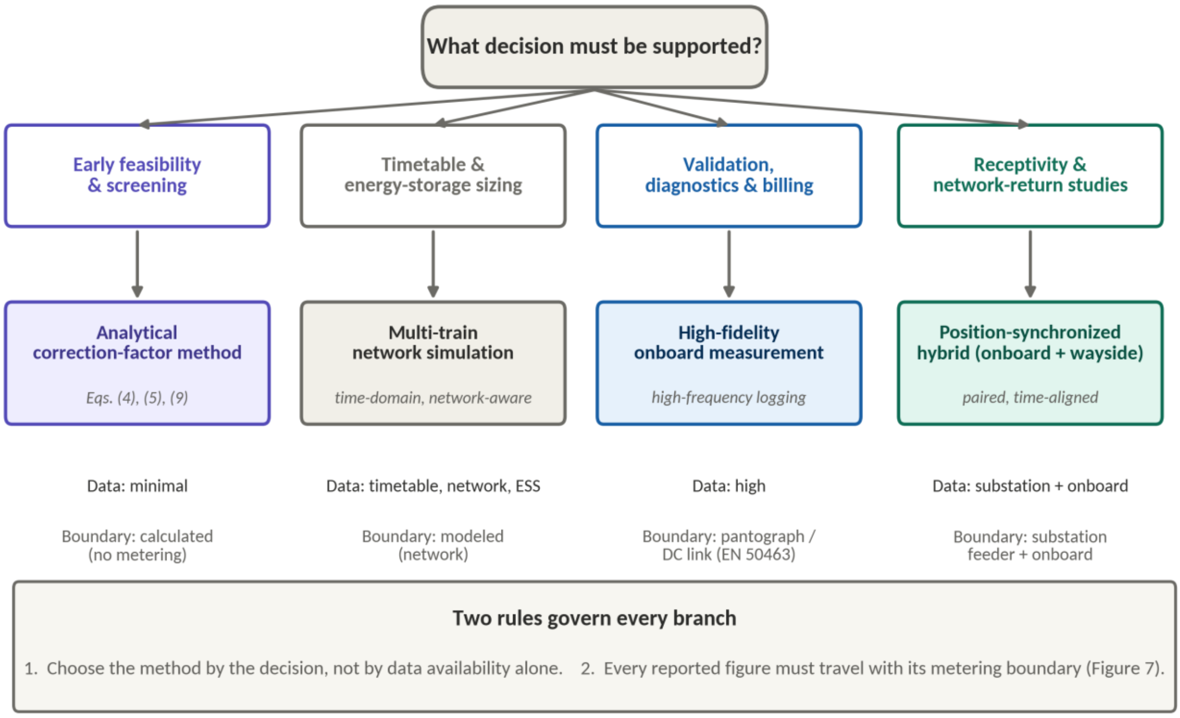

Fig. 9. Method and metering-boundary selection by decision context, operationalizing Table 5 and the two practical rules of Section 3.8. Each decision routes to a recommended method, its data requirement, and the metering boundary at which the resulting figure should be reported

4. Conclusions

This review has examined the calculation and measurement options for the two energy quantities that dominate the dynamic electricity balance of electric railway traction – acceleration energy and regenerative (recuperated) braking energy – for electric locomotives and EMUs, across AC and DC supply systems. Five conclusions stand out.

First, calculation and measurement are complementary and mutually dependent. For acceleration energy, the correction-factor method bridges the two: empirically determined factors ($\alpha_1 \approx 1.30$ for the kinetic-energy route and $\alpha_2 \approx 1.32$ for the traction-force route, cited here as representative case-specific values for Taurus 0470 intercity trains) reconcile physics-based calculation with measurement to within a few percent, provided the effective mass and a speed- and load-dependent efficiency are respected. The factor, however, is condition-dependent: aging rolling stock has shown deviations of tens of percent, so the factor must be revalidated rather than treated as a constant.

Second, measurement fidelity is governed by the metering boundary and sampling rate. Measurement technology for acceleration energy has progressed from dedicated traction-measuring cars to onboard logging, OCR from display, inertial sensors, and machine-learning estimation, trading fidelity for cost and intrusiveness. For regenerative energy, wayside measurement alone underestimates recovery on DC systems because it misses locally consumed energy, whereas high-frequency, position-synchronized hybrid measurement serves as the reference for validation.

Third, for regenerative braking, the binding constraint is receptivity, not availability. Utilized energy is limited by DC voltage-rise thresholds or AC phase synchronization, by the temporal overlap of braking and accelerating trains, and by the presence of reversible substations and storage. Measurement series on Hungarian lines indicate that recoverable regenerative energy is roughly 20–

30% of the energy consumed, with driving style and the placement of speed restrictions as first-order influences.

Fourth, the human operator is a measurable, non-negligible source of variability: disaggregating the acceleration-energy correction factor by driver shows it is not driver-independent, with per-event ratios ranging from sub-unity to well above the global median and a directional asymmetry exceeding a third of the baseline for one driver (present author, forthcoming), a magnitude comparable to traction-conversion losses.

Fifth, system type and vehicle architecture systematically shape outcomes: AC and DC systems face different dominant constraints, and distributed-traction EMUs recover more efficiently than locomotive-hauled trains.

On this basis, the review recommends: for measurement, high-frequency, position-synchronised acquisition with an explicitly documented metering boundary, and hybrid onboard-plus-wayside measurement for validation and storage sizing; for calculation, selection of the method by purpose – analytical for feasibility, multi-train simulation for timetable and storage decisions, data-driven only where large, well-curated datasets exist – always including voltage-rise and receptivity constraints and train-specific efficiency data; operationally, exhausting timetable and driving-strategy optimisation, supported by DAS and ATO, before investing in hardware; and, for the field as a whole, convergence on standardised metrics and reporting. Future work indicated by the corpus includes integrating driver-specific data (in compliance with data-protection requirements), simultaneously treating gradient, load, and timetable, evaluating higher-braking-force locomotives and storage technologies matched to the load spectrum, and implementing infrastructure measures such as selective double-tracking. Accurate, boundary-explicit measurement and purpose-matched calculation of acceleration and regenerative energy are prerequisites for realizing the energy-saving potential of electrified rail.

Limitations and Future Work

Three limitations qualify this synthesis. First, the present work is a structured narrative review rather than a systematic one, so the corpus, although broad and current, is not the product of an exhaustive, reproducible search; relevant studies may be missing, and the selection reflects topical and quality judgments. Second, the quantitative backbone of the acceleration-energy strand draws substantially on a single internally consistent measurement program for Hungarian and neighboring lines, so its correction factors and specific-energy values are best read as illustrative anchors pending broader cross-validation. Third, several headline regenerative-energy figures originate from single or secondary sources under specific metering boundaries and are reported as such rather than as established constants. Building on these limits, the most valuable next steps are multi-operator and multi-vehicle revalidation of the acceleration-energy correction factors; standardized, high-frequency, position-synchronized metering referenced to a common (EN 50463 [94]) boundary; broader AC/DC and locomotive/EMU datasets for regeneration and receptivity; mixed-effects driver models that treat the operator as an explicit covariate rather than as measurement noise; and uncertainty quantification for machine-learning estimators before they inform energy-management decision-making. Finally, the calculation-measurement framework set out here is not confined to catenary-fed stock: as railways decarbonize beyond the electrified network, the same accounting applies to battery-electric locomotives now entering heavy-haul freight service [98] and to hydrogen fuel-cell multiple units, whose technology status and on-board energy-management options are surveyed in recent reviews [99] and whose coupled energy and thermal management is increasingly optimized by data-driven, for instance deep-reinforcement-learning, controllers [100]; extending acceleration- and braking-energy measurement and correction-factor methods to these traction types is a natural and timely direction.

A further set of limitations is intrinsic to the calculation methods themselves rather than to the corpus. The analytical correction-factor and quasi-static energy-balance methods that underpin most of the reviewed estimates condense drivetrain conversion losses, auxiliary demand, running resistance, and adhesion variability into a small number of lumped parameters and assume a representative, speed- and load-dependent efficiency; they reproduce event-integrated energy accurately but, by construction, do not resolve instantaneous power or the underlying loss mechanisms, and their accuracy degrades whenever a lumped contributor shifts away from its calibrated value. Rolling-stock wear and ageing are one such contributor: progressive wheel-rail and mechanical wear, bearing and gear degradation, and the ageing of traction and auxiliary equipment raise running resistance and lower conversion efficiency over a vehicle's life, so a correction factor or specific-energy value calibrated on one fleet condition drifts with wear – for aged stock the literature reports deviations of tens of percent – which is why such factors must be periodically revalidated rather than treated as constants. The energy-accounting framework likewise abstracts away the fast electrical dynamics at the traction-to-recuperation transition: the pronounced current surges and the electromagnetic-compatibility (EMC) constraints that arise when a drive reverses power flow – converter current and voltage ratings, protection thresholds, and harmonic and EMC limits – can curtail the instantaneous recoverable power, yet they are represented only in dedicated power-electronic and EMC models and fall outside the energy-balance methods surveyed here. Finally, the traction supply network is nonlinear and time-varying: line receptivity depends on the instantaneous catenary or third-rail voltage, on substation rectifier and inverter characteristics, on line impedance, and on the simultaneous demand of other trains, so methods that adopt a fixed conversion efficiency or a constant voltage-rise threshold necessarily linearise a fundamentally nonlinear system. Multi-train power-flow simulation captures this nonlinearity more faithfully than closed-form analytical estimates, at the cost of substantially greater data and computational requirements. Recognizing these method-level limitations bounds the interpretation of the quantitative figures reported throughout and motivates coupling the energy-accounting methods reviewed here with power-systems and EMC modeling whenever instantaneous behavior, rather than event-integrated energy, is the quantity of interest.

Acknowledgement
This paper was supported by the János Bolyai Research Scholarship of the Hungarian Academy of Sciences. The paper was technically supported by the SZE-RAIL Research Team. The author expresses his deepest respect for the technical support of Raaberbahn Hungary, in particular Endre Lőkkös and Bálint Huszár, and is grateful to the locomotive drivers of the GYSEV (ROeEE) intercity services who consented to the cab-side measurement campaign during their regular duties. The author expresses gratitude for the help and technical support of Dr. Szabolcs Kocsis Szürke, Dr. Szabolcs Szalai, and Bence Hermán, colleagues at the Széchenyi István University; as well as the author's student groups at Széchenyi István University and Budapest University of Technology and Economics for their enthusiastic work and effort.

Declaration on the Use of Artificial Intelligence Tools
During the preparation of this manuscript, the author used Grammarly and DeepL solely for language editing and proofreading.

Conflicts of Interest

The author declares no conflicts of interest.

References

[1] Aroso, A., & Bugarín, M. R. (2024). Energy efficiency improvement on railway lines: An overview. *Energy Science & Engineering*, 12, 5753–5764. https://doi.org/10.1002/ese3.1971

[2] Al-lami, A., & Török, Á. (2025). Decomposition of carbon dioxide (CO2) emissions in Hungary: A case study based on the Kaya identity and LMDI model. *Periodica Polytechnica Transportation Engineering*, 53(1), 7–15. https://doi.org/10.3311/PPtr.37552

[3] Zöldy, M., Baranyi, P., & Török, Á. (2024). Trends in cognitive mobility in 2022. *Acta Polytechnica Hungarica*, 21(7), 189–202. https://doi.org/10.12700/APH.21.7.2024.7.11

[4] Wang, Y. Z., Zhou, S., & Ou, X. M. (2021). Development and application of a life cycle energy consumption and CO_2 emissions analysis model for high-speed railway transport in China. *Advances in Climate Change Research*, 12(2), 270–280. https://doi.org/10.1016/j.accre.2021.03.002

[5] Minaminosono, K., Hashimoto, M., & Yoshinaga, T. (2019). Study of potential and utilization of regenerative power in electric railway. In *8th International Conference on Renewable Energy Research and Applications (ICRERA)* (pp. 164–168). IEEE. https://doi.org/10.1109/ICRERA47325.2019.8996583

[6] Cipek, M., Pavković, D., Krznar, M., Kljaić, Z., & Mlinarić, T. J. (2021). Comparative analysis of conventional diesel-electric and hypothetical battery-electric heavy haul locomotive operation. *Energy*, 232, 121097. https://doi.org/10.1016/j.energy.2021.121097

[7] Naldini, F., Pellegrini, P., & Rodriguez, J. (2022). Real-time optimization of energy consumption in railway networks. *Transportation Research Procedia*, 62, 35–42. https://doi.org/10.1016/j.trpro.2022.02.005

[8] Barone, G., Buonomano, A., Forzano, C., Giuzio, G. F., Palombo, A., & Russo, G. (2025). An innovative waste heat recovery solution for HVAC systems in railway coaches. *Energy Reports*, 13, 5653–5661. https://doi.org/10.1016/j.egyr.2025.05.009

[9] Taran, I., & Moroz, D. (2024). Improving the efficiency of management of transport and energy resources of the logistics system of an industrial enterprise. *Naukovyi Visnyk Natsionalnoho Hirnychoho Universytetu*, (6), 143–150. https://doi.org/10.33271/nvngu/2024-6/143

[10] Fischer, S. (2015). Traction energy consumption of electric locomotives and electric multiple units at speed restrictions. *Acta Technica Jaurinensis*, 8(3), 240–256. https://doi.org/10.14513/actatechjaur.v8.n3.384

[11] Hamada, A. T., & Orhan, M. F. (2022). An overview of regenerative braking systems. *Journal of Energy Storage*, 52, 105033. https://doi.org/10.1016/j.est.2022.105033

[12] Lin, L., You, F., Lin, Y., Sun, T., & Huang, Y. (2025). Train regenerative braking energy management strategy considering battery state of charge. *Sustainable Energy, Grids and Networks*, 43, 101786. https://doi.org/10.1016/j.segan.2025.101786

[13] Rochard, B. P., & Schmid, F. (2000). A review of methods to measure and calculate train resistances. *Proceedings of the Institution of Mechanical Engineers, Part F: Journal of Rail and Rapid Transit*, 214(4), 185–199. https://doi.org/10.1243/0954409001531306

[14] Ihme, J. (2022). Running resistances of rail vehicles. In *Rail Vehicle Technology* (pp. 31–50). Springer. https://doi.org/10.1007/978-3-658-36969-9

[15] Bestard, M., Lindgreen, E. B., & Stichel, S. (2023). Monitoring energy usage of heavy-haul iron ore trains with on-board energy meter for improving energy efficiency. *Railway Sciences*, 2(2), 243–256. https://doi.org/10.1108/RS-04-2023-0020

[16] Hu, H., Liu, Y., Li, Y., He, Z., Gao, S., Zhu, X., & Tao, H. (2024). Traction power systems for electrified railways: Evolution, state of the art, and future trends. *Railway Engineering Science*, 32(1), 1–19. https://doi.org/10.1007/s40534-023-00320-6

[17] Liu, R., & Golovitcher, I. M. (2003). Energy-efficient operation of rail vehicles. *Transportation Research Part A: Policy and Practice*, 37(10), 917–932. https://doi.org/10.1016/j.tra.2003.07.001

[18] Fischer, S., Hermán, B., & Kocsis Szürke, S. (2025). Possibilities for determining the energy consumption of electric locomotives during acceleration and constant-speed traction. *Cognitive Sustainability*, 3(2), 154. https://doi.org/10.55343/CogSust.154

[19] Negrean, I., Crișan, A., Șerdean, F., & Vlase, S. (2022). New formulations on kinetic energy and acceleration energies in applied mechanics of systems. *Symmetry*, 14(5), 896. https://doi.org/10.3390/sym14050896

[20] Stojanović, V., Dimitrov, L., Tomov, P., Li, D., & Nikolić, V. (2024). Dynamic stability analysis of a coupled moving bogie system. *Facta Universitatis, Series: Mechanical Engineering*, 22(4), 773–785. https://doi.org/10.22190/FUME241003045S

[21] Alic, D., Matijošius, J., & Kilikevičius, A. (2025). Numerical modelling of the crosswind influence on vehicle aerodynamics in highway traffic conditions. *Facta Universitatis, Series: Mechanical Engineering*, 23(1), 65–77. https://doi.org/10.22190/FUME241212009A

[22] Fu, C., Sun, P., Zhang, J., Yan, K., Wang, Q., & Feng, X. (2023). An energy-efficient train control approach with dynamic efficiency of the traction system. *IET Intelligent Transport Systems*, 17(6), 1182–1199. https://doi.org/10.1049/itr2.12351

[23] Nold, M., & Corman, F. (2024). Increasing realism in modelling energy losses in railway vehicles and their impact to energy-efficient train control. *Railway Engineering Science*, 32(3), 257–285. https://doi.org/10.1007/s40534-023-00322-4

[24] Alberti, F., D'Andrea, D., Macor, A., Risitano, G., Rosseti, A., & Sedmak, A. (2024). Novel smart design of rear half shaft of large urban transport vehicle. *Facta Universitatis, Series: Mechanical Engineering*, 22(4), 583–599. https://doi.org/10.22190/FUME240203027A

[25] Kalmaganbetov, S. A., Isametova, M., Troha, S., Vrcan, Ž., Marković, K., & Marinković, D. (2024). Selection of optimal planetary transmission for light electric vehicle main gearbox. *Journal of Applied and Computational Mechanics*, 10(4), 742–753. https://doi.org/10.22055/JACM.2024.46280.4490

[26] Mandić, M., Uglešić, I., & Milardić, V. (2009). Electric railway power consumption. *Journal of Energy – Energija*, 58(4), 384–407. https://doi.org/10.37798/2009584306

[27] Scheepmaker, G. M., Goverde, R. M. P., & Kroon, L. G. (2017). Review of energy-efficient train control and timetabling. *European Journal of Operational Research*, 257(2), 355–376. https://doi.org/10.1016/j.ejor.2016.09.044

[28] Wang, J., & Rakha, H. A. (2017). Electric train energy consumption modeling. *Applied Energy*, 193, 346–355. https://doi.org/10.1016/j.apenergy.2017.02.005

[29] Zhou, F.-R., Zhou, K., Zhang, D., & Peng, Q.-Y. (2024). Optimization of the cruising speed for high-speed trains to reduce energy consumed by motion resistances. *Applied Energy*, 374, 124223. https://doi.org/10.1016/j.apenergy.2024.124223

[30] Panchenko, S., Gerlici, J., Lovska, A., Ravlyuk, V., Dižo, J., & Blatnický, M. (2024). Analysis of asymmetric wear of brake pads on freight wagons despite full contact between pad surface and wheel. *Symmetry*, 16(3), 346. https://doi.org/10.3390/sym16030346

[31] Iliev, I., Suslov, K., Kryukov, A., Cherepanov, A., Beloev, I., & Valeeva, Y. (2024). Modeling of energy recovery processes in railway traction power supply systems. *Energy Reports*, 11, 5163–5171. https://doi.org/10.1016/j.egyr.2024.05.012

[32] Mariscotti, A., Giordano, D., & Signorino, D. (2023). Energy efficiency improvement with reversible substations for electrified transportation systems. *The Open Transportation Journal*, 17, e187447782301091. https://doi.org/10.2174/18744478-v17-e230109-2022-13

[33] Wu, L., & Wu, M. (2024). Utilisation of regenerative braking energy in adjacent power sections of railway systems. *IET Electric Power Applications*, 18, 174–184. https://doi.org/10.1049/elp2.12378

[34] Fischer, S. (2026). Empirical observation of the influence of locomotive driver style on the acceleration-energy correction factor of Hungarian InterCity trains. In *Proceedings of the CogMob 2026 Conference* (in press).

[35] Bulakh, M. (2025). Evaluation and reduction of energy consumption of railway train movement on a straight track section with reduced freight wagon mass. *Energies*, 18(2), 280. https://doi.org/10.3390/en18020280

[36] González-Gil, A., Palacin, R., Batty, P., & Powell, J. P. (2014). A systems approach to reduce urban rail energy consumption. *Energy Conversion and Management*, 80, 509–524. https://doi.org/10.1016/j.enconman.2014.01.060

[37] Pineda-Jaramillo, J., Martínez-Fernández, P., Villalba-Sanchis, I., Salvador-Zuriaga, P., & Insa-Franco, R. (2021). Predicting the traction power of metropolitan railway lines using different machine learning models. *International Journal of Rail Transportation*, 9(5), 461–478. https://doi.org/10.1080/23248378.2020.1829513

[38] Urbaniak, M., Myrcik, J., Juda, M., & Mandrysz, J. (2025). The application of mobile devices for measuring accelerations in rail vehicles: Methodology and field research outcomes in tramway transport. *Sensors*, 25(15), 4635. https://doi.org/10.3390/s25154635

[39] Tudor, E., Vasile, I., Lipcinski, D., Dumitru, C., Tănase, N., Drăghici, F., & Popa, G. (2025). Accelerometers in monitoring systems for rail vehicle applications: A literature review. *Applied System Innovation*, 8(3), 70. https://doi.org/10.3390/asi8030070

[40] Ren, J., Zhang, Q., & Liu, F. (2020). Analysis of factors affecting traction energy consumption of electric multiple unit trains based on data mining. *Journal of Cleaner Production*, 262, 121374. https://doi.org/10.1016/j.jclepro.2020.121374

[41] Liang, H., Zhang, Y., Yang, P., Wang, L., & Gao, C. (2023). Comparison and analysis of prediction models for locomotive traction energy consumption based on the machine learning. *IEEE Access*, 11, 38502–38513. https://doi.org/10.1109/ACCESS.2023.3268531

[42] Tao, X., Sun, P., Xiao, Z., Fu, C., Feng, X., & Wang, Q. (2024). Modeling and energy-optimal control for freight trains based on data-driven approaches. *Future Generation Computer Systems*, 152, 346–360. https://doi.org/10.1016/j.future.2023.11.006

[43] Dawod, A. B. A., & Terdik, G. (2024). Use of zero-crossings segmentation for track quality assessment. *Acta Technica Jaurinensis*, 17(1), 8–21. https://doi.org/10.14513/actatechjaur.00726

[44] Istomin, S. (2018). The use of correlation and regression analysis for assessment of the energy effectiveness of the DC electric locomotives auxiliary equipment. *MATEC Web of Conferences*, 239, 01038. https://doi.org/10.1051/matecconf/201823901038

[45] Jakubowski, A., Jarzębowicz, L., Bartłomiejczyk, M., Skibicki, J., Judek, S., Wilk, A., & Płonka, M. (2021). Modeling of electrified transportation systems featuring multiple vehicles and complex power supply layout. *Energies*, 14(24), 8196. https://doi.org/10.3390/en14248196

[46] Fernández, P., Zuriaga, P., Sanchis, I., & Franco, R. (2019). Neural networks for modelling the energy consumption of metro trains. *Proceedings of the Institution of Mechanical Engineers, Part F: Journal of Rail and Rapid Transit*, 234(7), 722–733. https://doi.org/10.1177/0954409719872789

[47] Hoo, D. S., Chua, K. H., Lim, Y. S., Morris, S., & Wang, L. (2024). Comparison of regenerative braking energy recovery of a DC third rail system under various operating conditions. *International Journal of Electrical Power & Energy Systems*, 155, 109575. https://doi.org/10.1016/j.ijepes.2023.109575

[48] Nkurunziza, J. M. V., Nizeyimana, J. D., & Turabimana, P. (2021). Quantitative estimation of railway vehicle regenerative energy saving: A case of Addis Ababa Light Rail Transit (AALRT). *International Journal of Engineering Technologies*, 7(1), 9–19. https://doi.org/10.19072/ijet.839666

[49] Wang, P., Zhu, Y., & Corman, F. (2022). Passenger-centric periodic timetable adjustment problem for the utilization of regenerative energy. *Computers & Industrial Engineering*, 172(A), 108578. https://doi.org/10.1016/j.cie.2022.108578

[50] Chen, J., Ge, Y., Wang, K., Hu, H., He, Z., Tian, Z., & Li, Y. (2023). Integrated regenerative braking energy utilization system for multi-substations in electrified railways. *IEEE Transactions on Industrial Electronics*, 70(1), 298–310. https://doi.org/10.1109/TIE.2022.3146563

[51] Ceraolo, M., Lutzemberger, G., Meli, E., Pugi, L., Rindi, A., & Pancari, G. (2018). Energy storage systems to exploit regenerative braking in DC railway systems. *Journal of Energy Storage*, 16, 269–279. https://doi.org/10.1016/j.est.2018.01.017

[52] Yuan, J., Peng, L., Zhou, H., Gan, D., & Qu, K. (2024). Recent research progress and application of energy storage system in electrified railway. *Electric Power Systems Research*, 226, 109893. https://doi.org/10.1016/j.epsr.2023.109893

[53] Zhang, J., Li, Y., Xie, H., & Li, B. (2020). Urban rail transit energy storage based on regenerative braking energy utilization. *Journal of Physics: Conference Series*, 1549, 042053. https://doi.org/10.1088/1742-6596/1549/4/042053

[54] Eltaweel, M., & Herfatmanesh, M. R. (2024). Enhancing vehicular performance with flywheel energy storage systems: Emerging technologies and applications. *Journal of Energy Storage*, 103, 114386. https://doi.org/10.1016/j.est.2024.114386

[55] Luo, J., Gao, S., Wei, X., & Tian, Z. (2024). Adaptive energy management strategy for high-speed railway hybrid energy storage system based on double-layer fuzzy logic control. *International Journal of Electrical Power & Energy Systems*, 156, 109739. https://doi.org/10.1016/j.ijepes.2023.109739

[56] Liu, J., Kong, L., Yi, M., Liu, T., Fang, Z., Xiong, B., Wang, H., & Zhang, Z. (2024). Coil spring booster: A single-channel regenerative braking system for tram in a sustainable city. *Sustainable Energy Technologies and Assessments*, 63, 103648. https://doi.org/10.1016/j.seta.2024.103648

[57] Riabov, I., Goolak, S., & Neduzha, L. (2024). An estimation of the energy savings of a mainline diesel locomotive equipped with an energy storage device. *Vehicles*, 6(2), 611–631. https://doi.org/10.3390/vehicles6020028

[58] Riabov, I., Demydov, O., Tykhonov, A., & Yahotin, V. (2025). Application of an energy storage device on a haulage diesel-electric locomotive used in quarry rail transport. *Proceedings of the Institution of Mechanical Engineers, Part F: Journal of Rail and Rapid Transit*. https://doi.org/10.1177/09544097251405134

[59] Hillmansen, S., & Roberts, C. (2007). Energy storage devices in hybrid railway vehicles: A kinematic analysis. *Proceedings of the Institution of Mechanical Engineers, Part F: Journal of Rail and Rapid Transit*, 221(1), 135–143. https://doi.org/10.1243/09544097JRRT99

[60] Barrero, R., Tackoen, X., & Van Mierlo, J. (2008). Improving energy efficiency in public transport: Stationary supercapacitor based energy storage systems for a metro network. In *2008 IEEE Vehicle Power and Propulsion Conference* (pp. 1–8). IEEE. https://doi.org/10.1109/VPPC.2008.4677491

[61] Khodaparastan, M., & Mohamed, A. (2019). Flywheel vs. supercapacitor as wayside energy storage for electric rail transit systems. *Inventions*, 4(4), 62. https://doi.org/10.3390/inventions4040062

[62] Liu, Y., Chen, M., Lu, S., Chen, Y., & Li, Q. (2018). Optimized sizing and scheduling of hybrid energy storage systems for high-speed railway traction substations. *Energies*, 11(9), 2199. https://doi.org/10.3390/en11092199

[63] Khodaparastan, M., Mohamed, A. A., & Brandauer, W. (2019). Recuperation of regenerative braking energy in electric rail transit systems. *IEEE Transactions on Intelligent Transportation Systems*, 20(8), 2831–2847. https://doi.org/10.1109/TITS.2018.2886809

[64] Domínguez, M., Fernández-Cardador, A., Fernández-Rodríguez, A., Cucala, A. P., Pecharromán, R. R., Urosa Sánchez, P., & Vadillo Cortázar, I. (2025). Review on the use of energy storage systems in railway applications. *Renewable and Sustainable Energy Reviews*, 207, 114904. https://doi.org/10.1016/j.rser.2024.114904

[65] Arboleya, P., Mohamed, B., & El-Sayed, I. (2020). Off-board and on-board energy storage versus reversible substations in DC railway traction systems. *IET Electrical Systems in Transportation*, 10(2), 185–195. https://doi.org/10.1049/iet-est.2019.0022

[66] Kleftakis, V. A., & Hatziargyriou, N. D. (2019). Optimal control of reversible substations and wayside storage devices for voltage stabilization and energy savings in metro railway networks. *IEEE Transactions on Transportation Electrification*, 5(2), 515–523. https://doi.org/10.1109/TTE.2019.2913355

[67] Teymourfar, R., Asaei, B., Iman-Eini, H., & Nejati fard, R. (2012). Stationary super-capacitor energy storage system to save regenerative braking energy in a metro line. *Energy Conversion and Management*, 56, 206–214. https://doi.org/10.1016/j.enconman.2011.11.019

[68] Şen, M., Özcan, M., & Eker, Y. R. (2024). Fuzzy logic-based energy management system for regenerative braking of electric vehicles with hybrid energy storage system. *Applied Sciences*, 14(7), 3077. https://doi.org/10.3390/app14073077

[69] Restel, F. J. (2024). A fuzzy-based method of assigning train managers to task types. *Cognitive Sustainability*, 3(4). https://doi.org/10.55343/CogSust.108

[70] Wang, P., & Goverde, R. M. P. (2019). Multi-train trajectory optimization for energy-efficient timetabling. *European Journal of Operational Research*, 272(2), 621–635. https://doi.org/10.1016/j.ejor.2018.06.034

[71] de Sousa, C. A., Pereira, S. L., & Guedes, R. S. (2024). Review and trends in regenerative braking energy recovery for traction power system with inverter substation in subways of São Paulo city. *Journal of Rail Transport Planning & Management*, 30, 100443. https://doi.org/10.1016/j.jrtpm.2024.100443

[72] Jiang, X., Hu, H., Yang, X., He, Z., Qian, Q., & Tricoli, P. (2019). Analysis and adaptive mitigation scheme of low-frequency oscillations in AC railway traction power systems. *IEEE Transactions on Transportation Electrification*, 5(3), 715–726. https://doi.org/10.1109/TTE.2019.2926571

[73] Popescu, M., & Bitoleanu, A. (2019). A review of the energy efficiency improvement in DC railway systems. *Energies*, 12(6), 1092. https://doi.org/10.3390/en12061092

[74] Xing, Z., Zhang, Z., Guo, J., Qin, Y., & Jia, L. (2023). Rail train operation energy-saving optimization based on improved brute-force search. *Applied Energy*, 330, 120345. https://doi.org/10.1016/j.apenergy.2022.120345

[75] Scheepmaker, G. M., Willeboordse, H. Y., Hoogenraad, J. H., Luijt, R. S., & Goverde, R. M. P. (2020). Comparing train driving strategies on multiple key performance indicators. *Journal of Rail Transport Planning & Management*, 13, 100163. https://doi.org/10.1016/j.jrtpm.2019.100163

[76] Habib, L., Oukacha, O., & Enjalbert, S. (2021). Towards tramway safety by managing advanced driver assistance systems depending on grades of automation. *IFAC-PapersOnLine*, 54(2), 227–232. https://doi.org/10.1016/j.ifacol.2021.06.026

[77] Sánchez-Contreras, G., Fernández-Rodríguez, A., Fernández-Cardador, A., & Cucala, A. P. (2023). A two-level fuzzy multi-objective design of ATO driving commands for energy-efficient operation of metropolitan railway lines. *Sustainability*, 15(12), 9238. https://doi.org/10.3390/su15129238

[78] Rodriguez, R., Trovão, J. P. F., & Solano, J. (2022). Fuzzy logic-model predictive control energy management strategy for a dual-mode locomotive. *Energy Conversion and Management*, 253, 115111. https://doi.org/10.1016/j.enconman.2021.115111

[79] Yang, X., Li, X., Ning, B., & Tang, T. (2016). A survey on energy-efficient train operation for urban rail transit. *IEEE Transactions on Intelligent Transportation Systems*, 17(1), 2–13. https://doi.org/10.1109/TITS.2015.2447507

[80] Wang, Y., De Schutter, B., van den Boom, T. J. J., & Ning, B. (2013). Optimal trajectory planning for trains – A pseudospectral method and a mixed integer linear programming approach. *Transportation Research Part C: Emerging Technologies*, 29, 97–114. https://doi.org/10.1016/j.trc.2013.01.007

[81] Allen, L., & Chien, S. (2021). Application of regenerative braking with optimized speed profiles for sustainable train operation. *Journal of Advanced Transportation*, 2021, 8555372. https://doi.org/10.1155/2021/8555372

[82] Huang, K., Liao, F., & Gao, Z. (2021). An integrated model of energy-efficient timetabling of the urban rail transit system with multiple interconnected lines. *Transportation Research Part C: Emerging Technologies*, 129, 103171. https://doi.org/10.1016/j.trc.2021.103171

[83] Guo, Y., & Zhang, C. (2022). Near real-time time-tabling for metro system energy optimization considering passenger flow and random delays. *Journal of Rail Transport Planning & Management*, 21, 100292. https://doi.org/10.1016/j.jrtpm.2022.100292

[84] Xu, Y., Jia, B., Li, X., Li, M., & Ghiasi, A. (2020). An integrated micro-macro approach for high-speed railway energy-efficient timetabling problem. *Transportation Research Part C: Emerging Technologies*, 112, 88–115. https://doi.org/10.1016/j.trc.2020.01.013

[85] Deng, L., Chen, M., Duan, K., Ouyang, L., & Shi, F. (2023). Integrated energy-efficient optimization for urban rail transit timetable. *IET Intelligent Transport Systems*, 17(9), 1819–1834. https://doi.org/10.1049/itr2.12368

[86] Li, J., Pan, F., Tong, S., Zhang, L., Li, X., & Yang, X. (2022). Energy-saving metro train timetable optimization method based on a dynamic passenger flow distribution. *Journal of Advanced Transportation*, 2022, 9776845. https://doi.org/10.1155/2022/9776845

[87] Liu, W., Su, S., Tang, T., & Wang, X. (2021). A DQN-based intelligent control method for heavy haul trains on long steep downhill section. *Transportation Research Part C: Emerging Technologies*, 129, 103249. https://doi.org/10.1016/j.trc.2021.103249

[88] He, D., Zhang, L., Guo, S., Chen, Y., Shan, S., & Jian, H. (2021). Energy-efficient train trajectory optimization based on improved differential evolution algorithm and multi-particle model. *Journal of Cleaner Production*, 304, 127163. https://doi.org/10.1016/j.jclepro.2021.127163

[89] Xing, Z., Zhu, J., Zhang, Z., Qin, Y., & Jia, L. (2022). Energy consumption optimization of tramway operation based on improved PSO algorithm. *Energy*, 258, 124848. https://doi.org/10.1016/j.energy.2022.124848

[90] Lai, Q., Liu, J., Haghani, A., Meng, L., & Wang, Y. (2020). Energy-efficient speed profile optimization for medium-speed maglev trains. *Transportation Research Part E: Logistics and Transportation Review*, 141, 102007. https://doi.org/10.1016/j.tre.2020.102007

[91] Yin, J., Ning, C., & Tang, T. (2022). Data-driven models for train control dynamics in high-speed railways: LAG-LSTM for train trajectory prediction. *Information Sciences*, 600, 377–400. https://doi.org/10.1016/j.ins.2022.04.004

[92] Suarez, J., Makridis, M., Anesiadou, A., Komnos, D., Ciuffo, B., & Fontaras, G. (2022). Benchmarking the driver acceleration impact on vehicle energy consumption and CO_2 emissions. *Transportation Research Part D: Transport and Environment*, 107, 103282. https://doi.org/10.1016/j.trd.2022.103282

[93] Pulvirenti, L., Tresca, L., Rolando, L., & Millo, F. (2022). Attention horizon as a predictor for the fuel consumption rate of drivers. *Sensors*, 22(5), 1801. https://doi.org/10.3390/s22051801

[94] EN 50463. (2017). *Railway applications – Energy measurement on board trains*. European Committee for Electrotechnical Standardization (CENELEC).

[95] EN 50388. (2012). *Railway applications – Power supply and rolling stock – Technical criteria for the coordination between power supply (substation) and rolling stock to achieve interoperability*. European Committee for Electrotechnical Standardization (CENELEC).

[96] EN 61375-2-6. (2018). *Electronic railway equipment – Train communication network (TCN) – Part 2-6: On-board to ground communication*. European Committee for Electrotechnical Standardization (CENELEC).

[97] EN 50591. (2019). *Railway applications – Rolling stock – Specification and verification of energy consumption*. European Committee for Electrotechnical Standardization (CENELEC).

[98] Lu, A., & Allen, J. G. (2024). Intermittent electrification with battery locomotives and the post-diesel future of North American freight railroads. *Transportation Research Record*. https://doi.org/10.1177/03611981241245996

[99] Ding, D., & Wu, X.-Y. (2024). Hydrogen fuel cell electric trains: Technologies, current status, and future. *Applications in Energy and Combustion Science*, 17, 100255. https://doi.org/10.1016/j.jaecs.2024.100255

[100] Jiang, K., Tian, Z., Wen, T., Song, K., Hillmansen, S., & Ochieng, W. Y. (2025). Collaborative optimization strategy of hydrogen fuel cell train energy and thermal management system based on deep reinforcement learning. *Applied Energy*, 393, 126057. https://doi.org/10.1016/j.apenergy.2025.126057